

Heavy Flavors:

Working with heavy quarks at High Scales & High Orders

Fred Olness

SMU

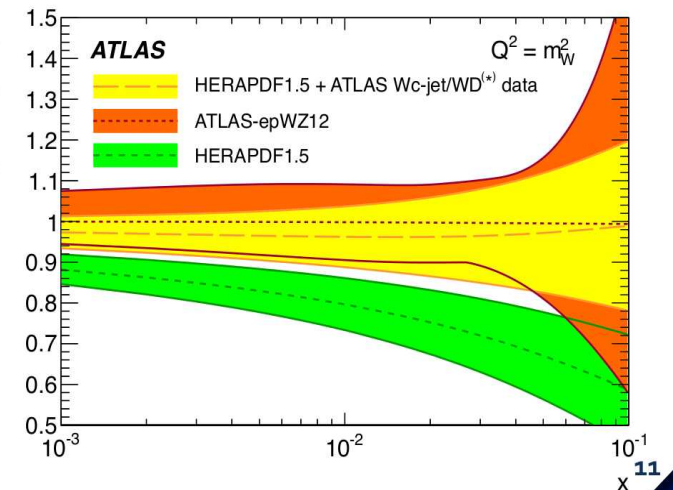
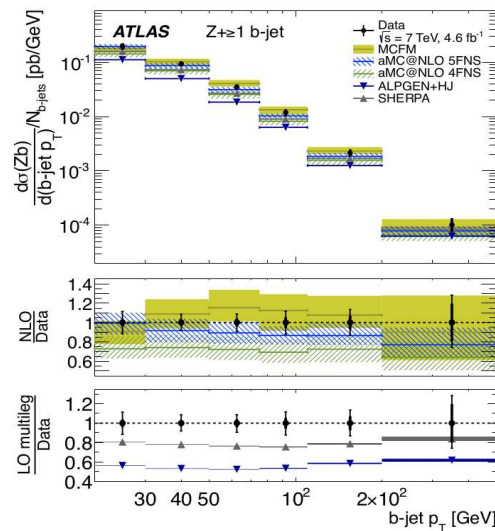
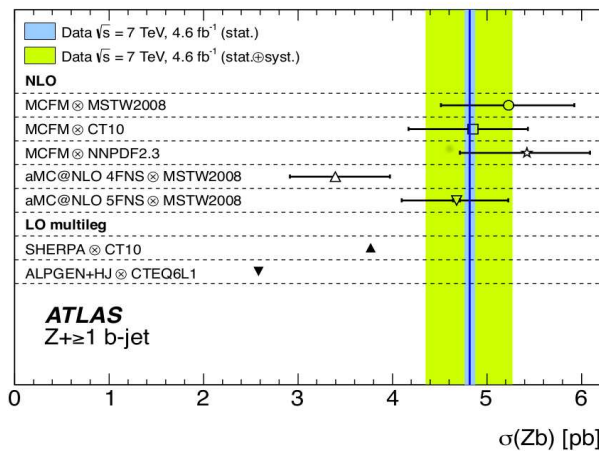
... informal discussion topics

- + Further sensitivity to s-quark content of the PDF from W+c studies
- + Two measurements strategies: tag the c-jet vs reconstruct D-meson
- + Consistently with W/Z inclusive measurements, ATLAS data favor s-quark enhancement against 1/2 suppression wrt d-quark PDF
 - Substantial reductions of uncertainty

Heavy flavor: Z+b-jets

JHEP 10 (2014) 141

- + Good agreement with NLO MCFM and aMC@NLO
 - Seems to favor scheme where b-quark is taken from PDF (5 FNS)
 - LO+PS generators are underestimating the cross section
 - Can't constrain PDF yet due to too large uncertainty
- + Good description of b-jet p_T shape
 - Normalization is off



The ACOT Scheme for heavy quarks PDFs

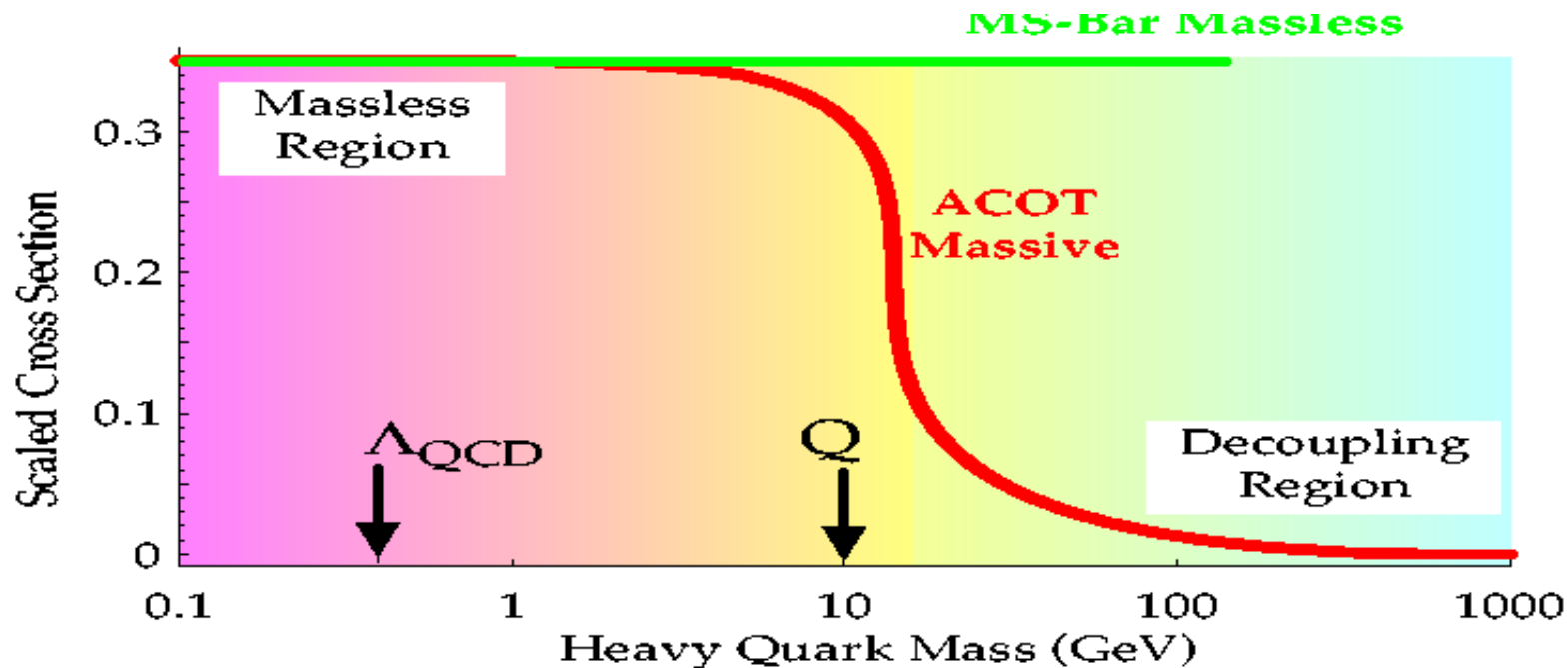
Theorists would much prefer that quark masses only come in 2 varieties:

$m = 0$: Massless case.

Mass plays no dynamic role
Well understood.

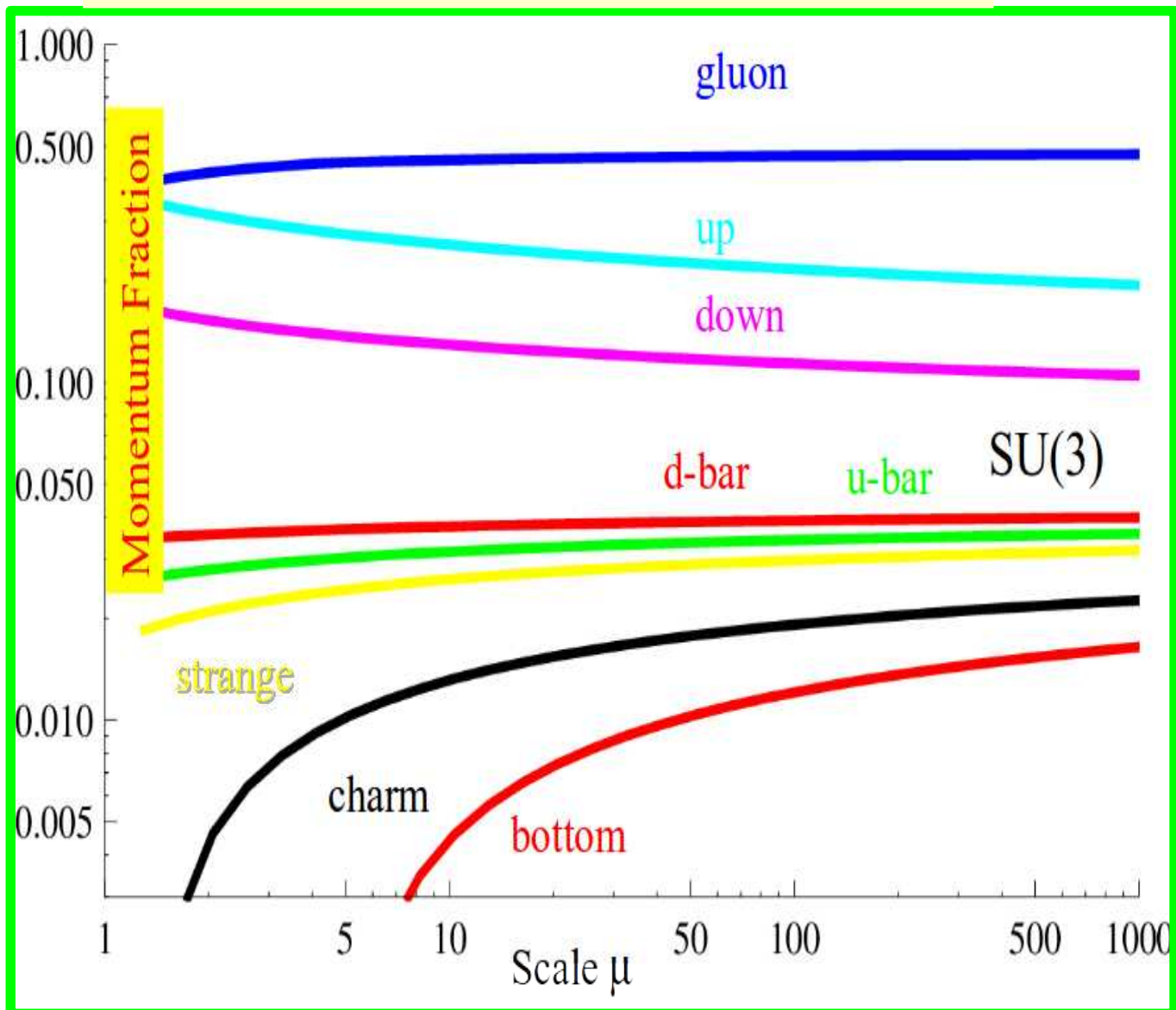
$m = \infty$: Infinite case.

Mass Decouples.
We can forget about this object

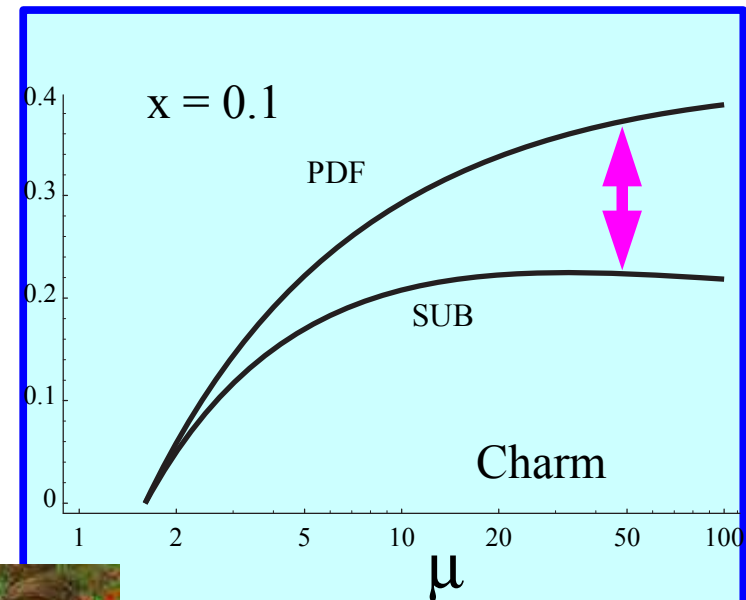
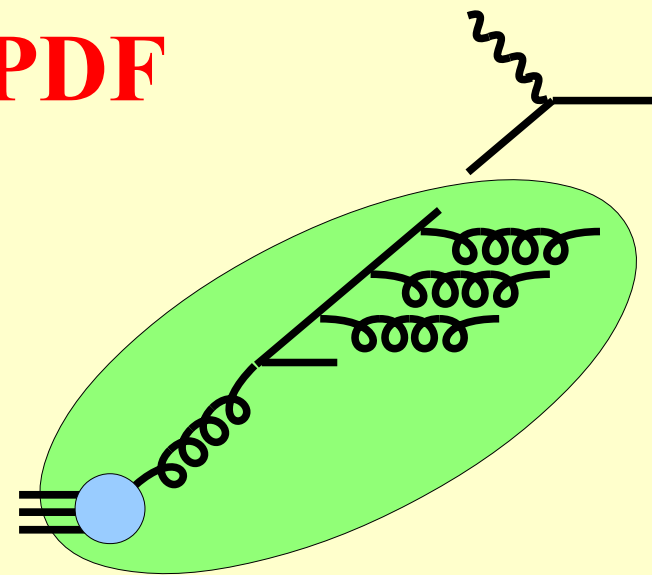


Charm & Bottom PDFs Resum Logs

Resum $\alpha_s \ln(m/Q)$

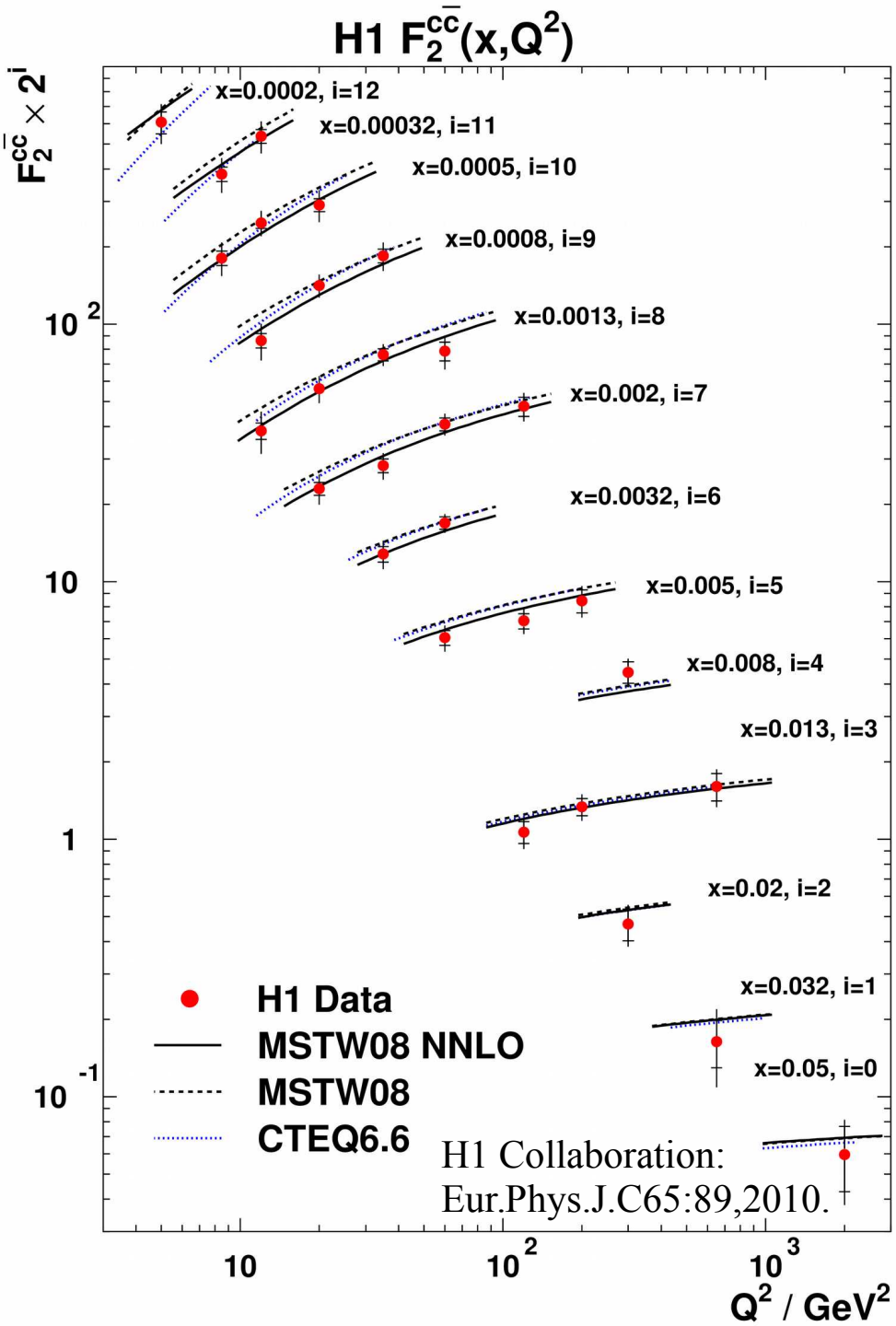


PDF

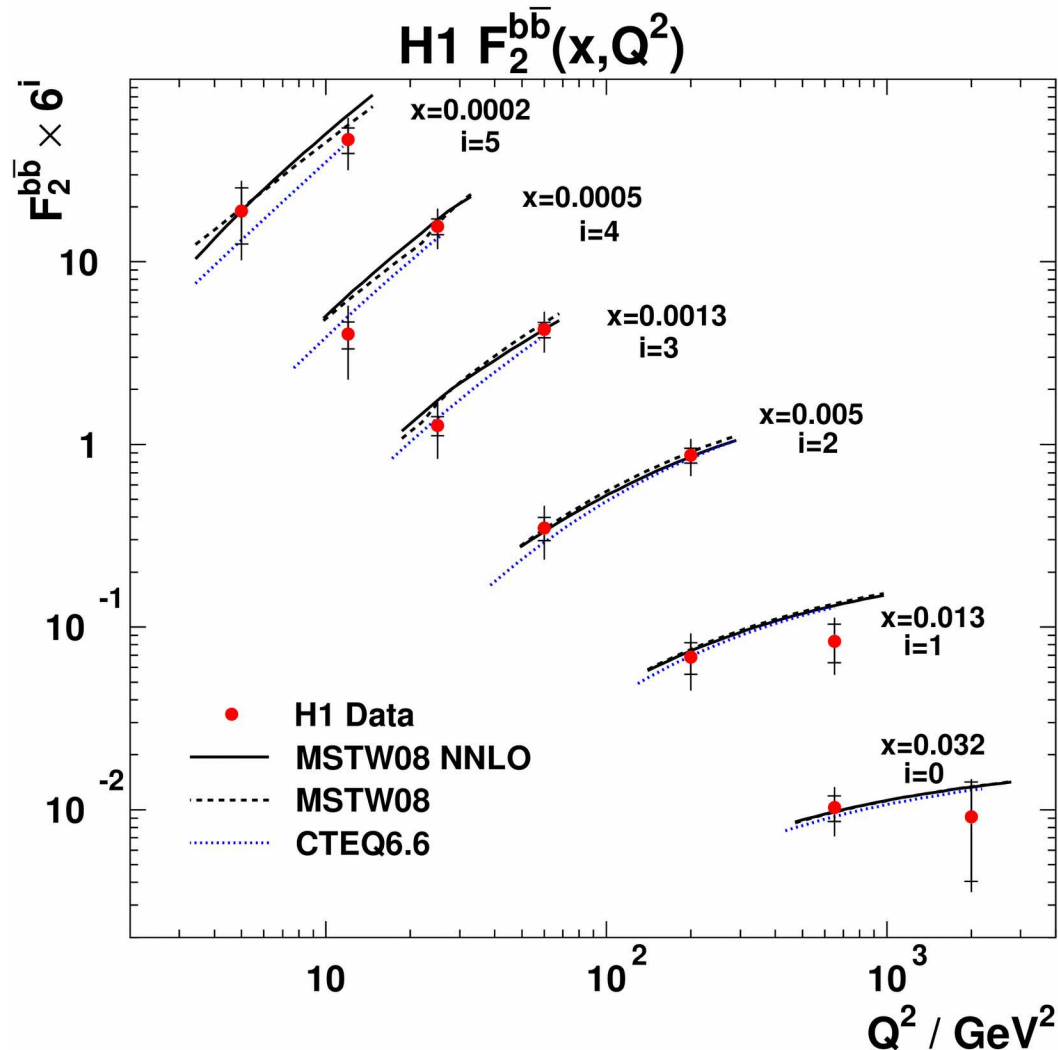
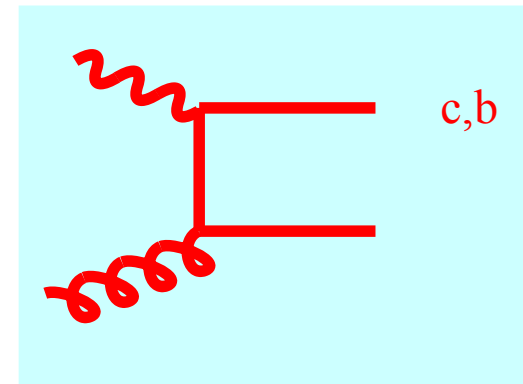


Plots made with ManeParse Mathematica package

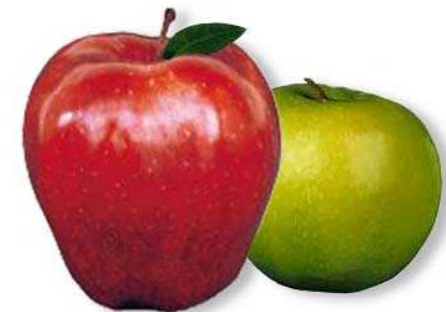
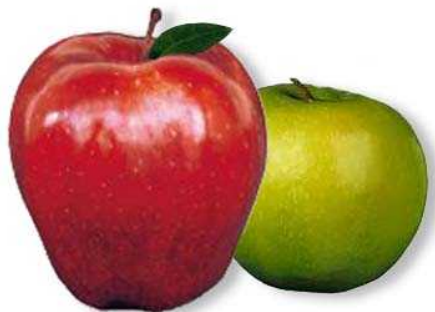




**c & b
tied to
gluon PDFs**



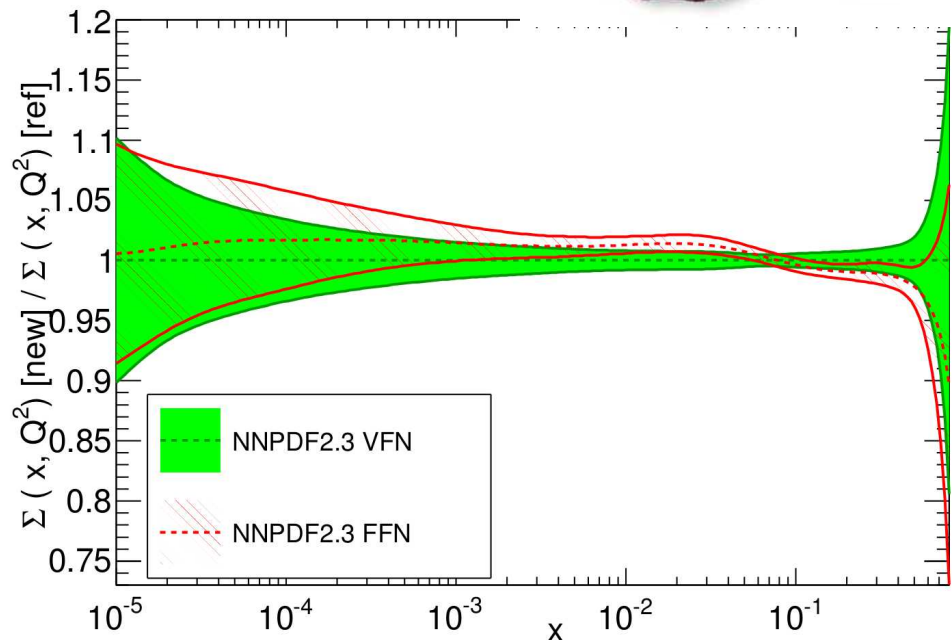
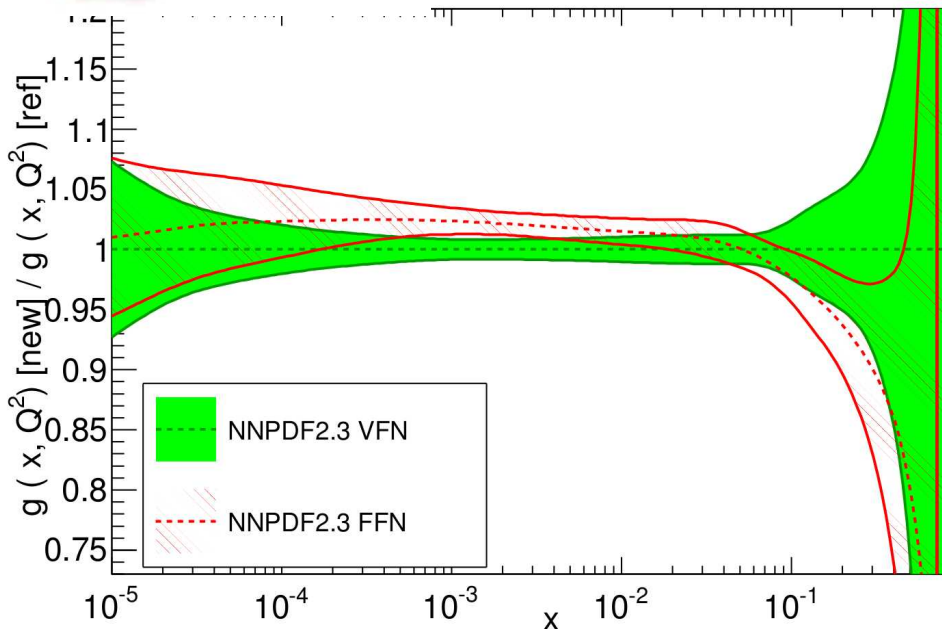
Compare VFN & FFN Schemes



Resum: $\propto \ln(m/Q)$

NNLO, $\alpha_s = 0.119$, $Q^2 = 10^4 \text{ GeV}^2$

Ratio to NNPDF2.3 NNLC



$$\Delta\chi^2 \equiv \chi_{FFN}^2 - \chi_{VFN}^2 > 0$$

x_{\min}	x_{\max}	Q_{\min}^2 (GeV)	Q_{\max}^2 (GeV)	$\Delta\chi^2$ (DIS)	$N_{\text{dat}}^{\text{DIS}}$	$\Delta\chi^2$ (HERA-I)	$N_{\text{dat}}^{\text{hera-I}}$
$4 \cdot 10^{-5}$	1	3	10^6	72.2	2936	77.1	592
$4 \cdot 10^{-5}$	0.1	3	10^6	87.1	1055	67.8	405
$4 \cdot 10^{-5}$	0.01	3	10^6	40.9	422	17.8	202
$4 \cdot 10^{-5}$	1	10	10^6	53.6	2109	76.4	537
$4 \cdot 10^{-5}$	1	100	10^6	91.4	620	97.7	412
$4 \cdot 10^{-5}$	0.1	10	10^6	84.9	583	67.4	350
$4 \cdot 10^{-5}$	0.1	100	10^6	87.7	321	87.1	227

General ideas & assumptions behind heavy quark PDF, ACOT, and VFNS

```
Order = 'NLO'          ! 'LO', 'NLO' or 'NNLO', used for DGLAP evolution.
```

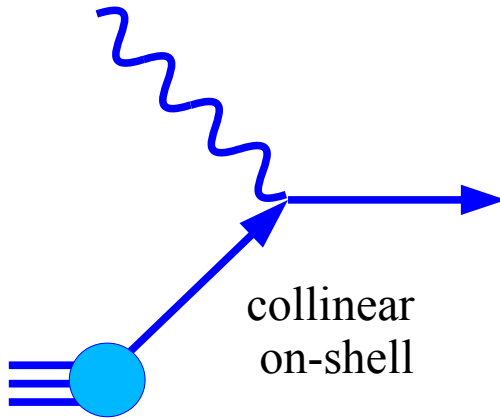
```
Q02      = 1.9 ! Evolution starting scale
```

```
! --- Scheme for heavy flavors
! --- HF_SCHEME = 'ZMVFNS'           : ZM-VFNS (massless) from QCDNUM,
! --- HF_SCHEME = 'ZMVFNS MELA'      : ZM-VFNS (massless) from MELA (N-space),
! --- HF_SCHEME = 'RT'               : Thorne-Roberts VFNS (massive)
! --- HF_SCHEME = 'RT FAST'          : Fast approximate TR VFNS scheme, usign k-factor
! --- HF_SCHEME = 'RT OPT'           : Thorne-Roberts VFNS (massive)
! --- HF_SCHEME = 'RT OPT FAST'      : Fast approximate TR VFNS scheme, usign k-factor
! --- HF_SCHEME = 'ACOT Full'        : ACOT - F.Olness Version (massive), using k-factors
! --- HF_SCHEME = 'ACOT Chi'         : ACOT - F.Olness Version (massive), using k-factors
! --- HF_SCHEME = 'ACOT ZM'          : ACOT - F.Olness Version (massless), using k-factors
! --- HF_SCHEME = 'FF'               : Fixed Flavour Number Scheme (qcdnum)
! --- HF_SCHEME = 'FF ABM'           : Fixed Flavour Number Scheme (ABM)
! --- HF_SCHEME = 'FF ABM RUNM'      : Fixed Flavour Number Scheme (ABM) using run mass def
! --- HF_SCHEME = 'FONLL-A'          : FONLL-A mass scheme provided by APFEL with pole masses (available only at NLO)
! --- HF_SCHEME = 'FONLL-A RUNM OFF' : FONLL-A mass scheme provided by APFEL with MSbar masses running OFF (available only at NLO)
! --- HF_SCHEME = 'FONLL-A RUNM ON'  : FONLL-A mass scheme provided by APFEL with MSbar masses running ON (available only at NLO)
! --- HF_SCHEME = 'FONLL-B'         : FONLL-B mass scheme provided by APFEL with pole masses (available only at NLO)
! --- HF_SCHEME = 'FONLL-B RUNM OFF' : FONLL-B mass scheme provided by APFEL with MSbar masses running OFF (available only at NLO)
! --- HF_SCHEME = 'FONLL-B RUNM ON'  : FONLL-B mass scheme provided by APFEL with MSbar masses running ON (available only at NLO)
! --- HF_SCHEME = 'FONLL-C'         : FONLL-C mass scheme provided by APFEL with pole masses (available only at NNLO)
! --- HF_SCHEME = 'FONLL-C RUNM OFF' : FONLL-C mass scheme provided by APFEL with MSbar masses running OFF (available only at NNLO)
! --- HF_SCHEME = 'FONLL-C RUNM ON'  : FONLL-C mass scheme provided by APFEL with MSbar masses running ON (available only at NNLO)
! (Any of the FONLL schemes at LO is equivalent to the ZM-VFNS)
```

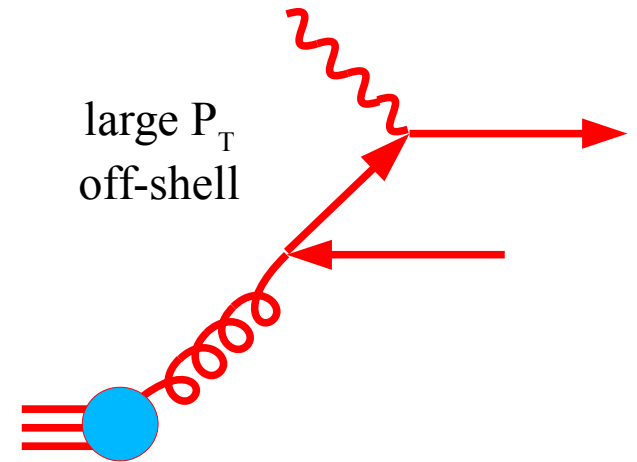
```
HF_SCHEME = 'RT FAST'
```

Wait a minute!

Since the heavy quark originally came from a gluon splitting, these diagrams are
Double Counting

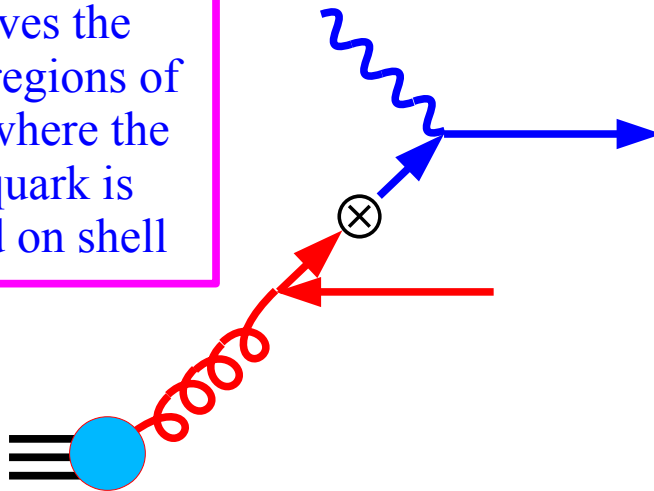


Leading Order (LO)



Next-to-Leading Order (NLO)

SUB removes the overlapping regions of phase space where the t-channel quark is collinear and on shell



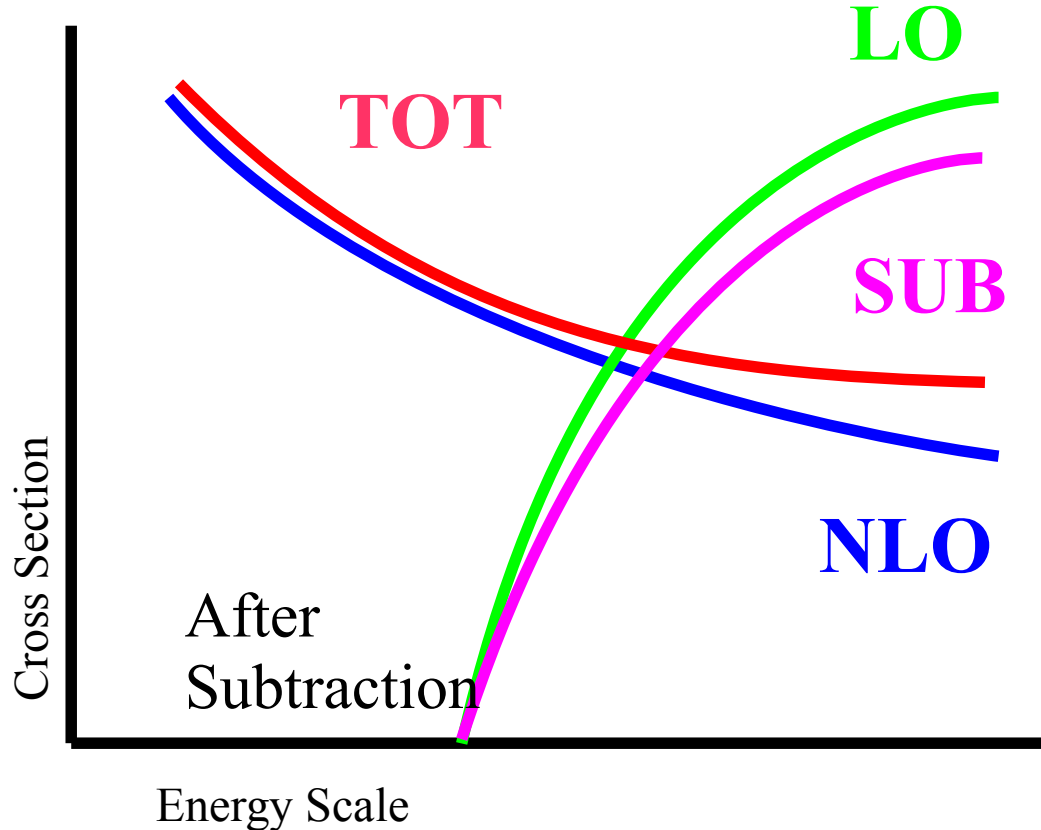
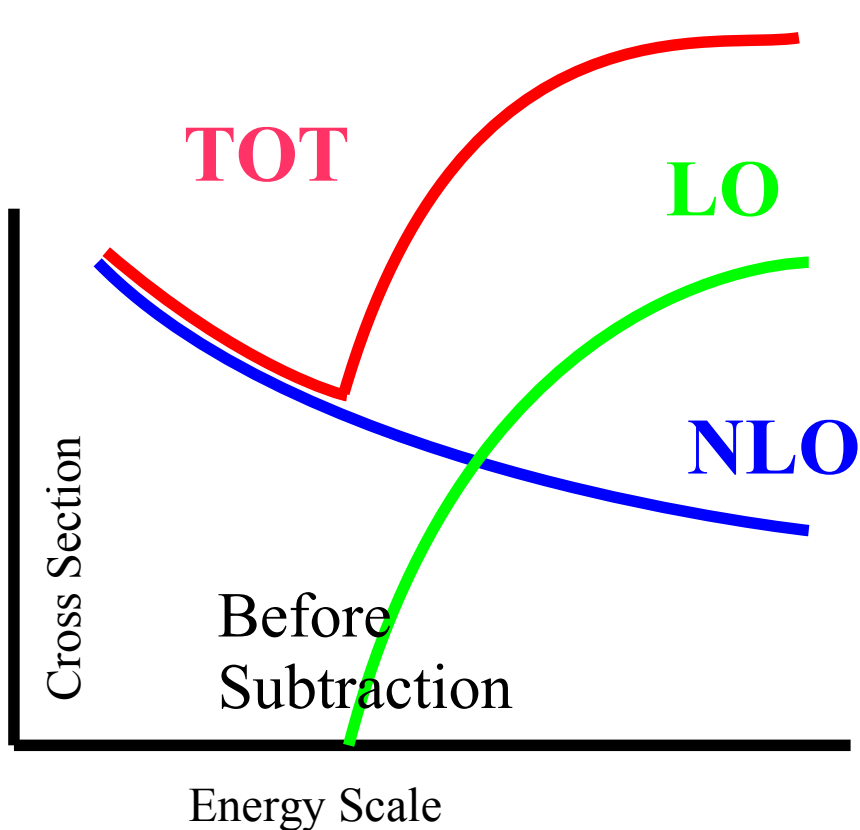
Subtraction (SUB)

$$\text{TOT} = \text{LO} + (\text{NLO} - \text{SUB})$$

Formally, NLO

Interaction of the separate contributions vs. energy scale

Note, we'll see this again ...



$$\text{TOT} = \text{LO} + \text{NLO} - \text{Subtraction (SUB)}$$

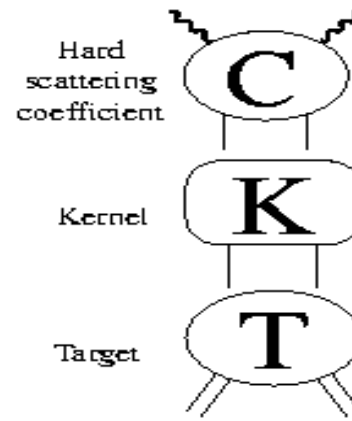
The diagram illustrates the components of the total cross section. On the left, a green wavy line (representing a photon) is connected to a green vertex, which then splits into two green lines. This is labeled 'LO'. In the middle, a blue wavy line is connected to a blue vertex, which then splits into two blue lines. This is labeled 'NLO'. On the right, a magenta wavy line is connected to a magenta vertex, which then splits into two magenta lines. This is labeled 'Subtraction (SUB)'. The overall equation is $\text{TOT} = \text{LO} + \text{NLO} - \text{Subtraction (SUB)}$.

There is a rigorous factorization proof ...

Ingredients of Factorization

Decompose into (t-channel) 2PI amplitudes:

$$\sigma = \sum_{N=1}^{\infty} C (K)^N T + \text{Non-leading}$$



A formal proof was constructed by numerous groups.

Collins, Soper, Sterman. *Perturbative QCD*, World Scientific (1989). Collins, in preparation

After reorganization of the infinite sum:

Parton Model

Remainder

$$\sigma \approx \underbrace{C [1 - (1-Z) K]^{-1} Z}_{\text{Wilson Coefficient (Hard Scatt. } \hat{\sigma})} \underbrace{[1 - K]^{-1} T}_{\text{Parton Distribution}} + \underbrace{C [1 - (1-Z) K]^{-1} (1-Z) T}_{\text{Power Suppressed}}$$

Z: collinear projection

This proof was explicitly extended to the case of massive quarks

(Collins, 1998)

Wilson Coefficient:

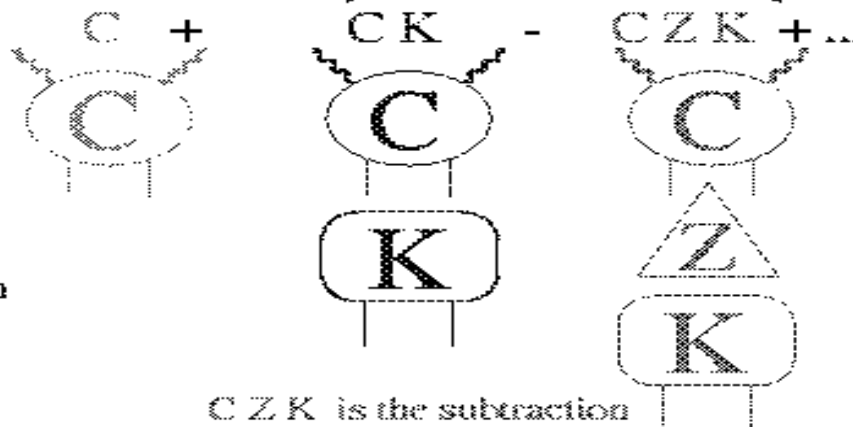
Leading Order

Next to Leading Order

$$C [1 - (1-Z) K]^{-1} \approx$$

All orders result

Wilson Coefficient:
IR safe "hard"
scattering cross section



C Z K is the subtraction

THOUGH EXPERIMENT
To keep things simple,
let's consider
scattering
off a parton target.

Application of Factorization Formula at Leading Order (LO)

Basic Factorization Formula

$$\sigma = f \otimes \omega + O(\Lambda^2/Q^2)$$

At Zeroth Order:

$$\sigma^0 = f^0 \otimes \omega^0 + O(\Lambda^2/Q^2)$$

Use: $f^0 = \delta$ for a parton target.

Therefore:

$$\sigma^0 = f^0 \otimes \omega^0 = \delta \otimes \omega^0 = \omega^0$$



f^0



f^1

for parton target

$$\sigma^0 = \omega^0$$

Warning: This trivial result leads to many misconceptions at higher orders

Application of Factorization Formula at Next to Leading Order (NLO)

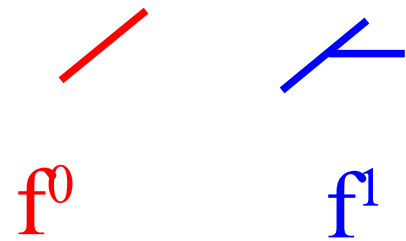
Basic Factorization Formula

$$\sigma = f \otimes \omega + O(\Lambda^2/Q^2)$$

At First Order:

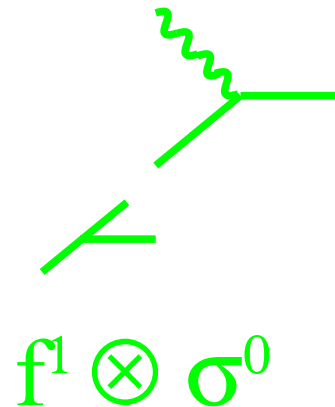
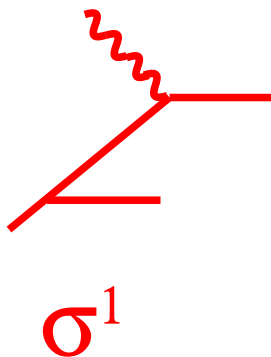
$$\begin{aligned}\sigma^1 &= f^1 \otimes \omega^0 + f^0 \otimes \omega^1 + \\ \sigma^1 &= f^1 \otimes \omega^0 + \omega^1\end{aligned}$$

We used: $f^0 = \delta$ and $d^0 = \delta$ for a parton target.



Therefore:

$$\omega^1 = \sigma^1 - f^1 \otimes \omega^0$$

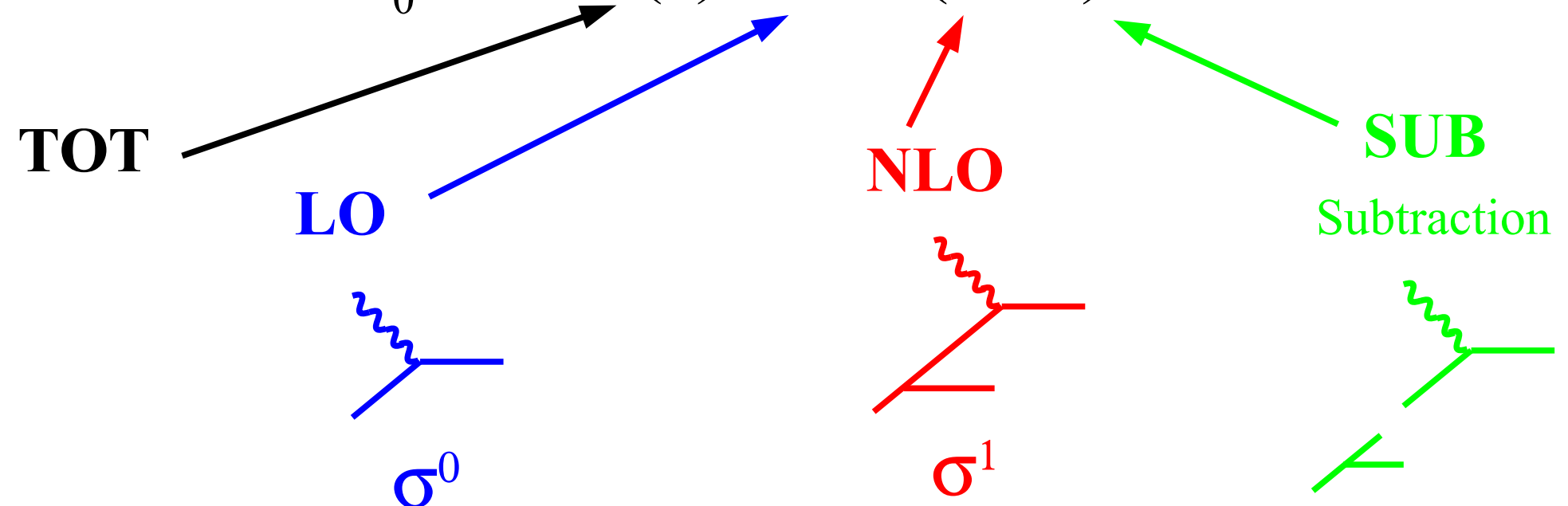


An Example: How the separate pieces can conspire

Expand $f(x)=x$ in Taylor Series about x_0 .

$$\text{For } x_0=0: \quad f(\varepsilon) = 0 + (\varepsilon - 0) + \dots = \varepsilon$$

$$\text{For } x_0=1: \quad f(\varepsilon) = 1 + (\varepsilon - 1) + \dots = \varepsilon$$



$$\text{TOT} = \text{LO} + \text{NLO} - \text{SUB}$$

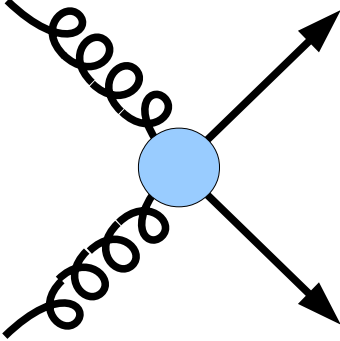
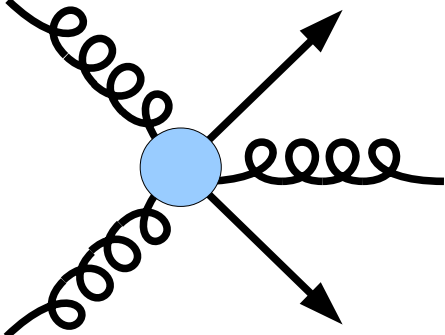
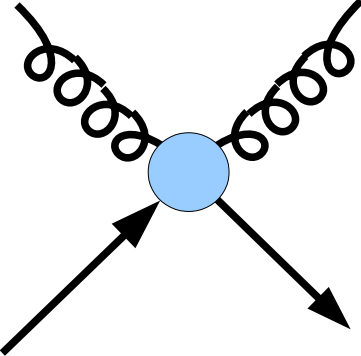
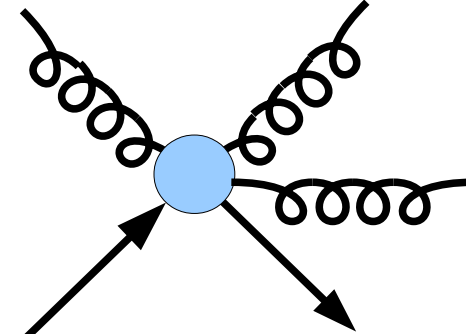
The Moral

**It doesn't matter which expansion point you use;
QCD will compensate (if you go to high enough
order).**

In practice ...

**we are often limited to low-order calculations,
so it is wise to choose your expansion point carefully.**

The Basic Contributions to Heavy Flavor Production

	Leading Order	Next to LO
Heavy Creation		
Heavy Excitation		

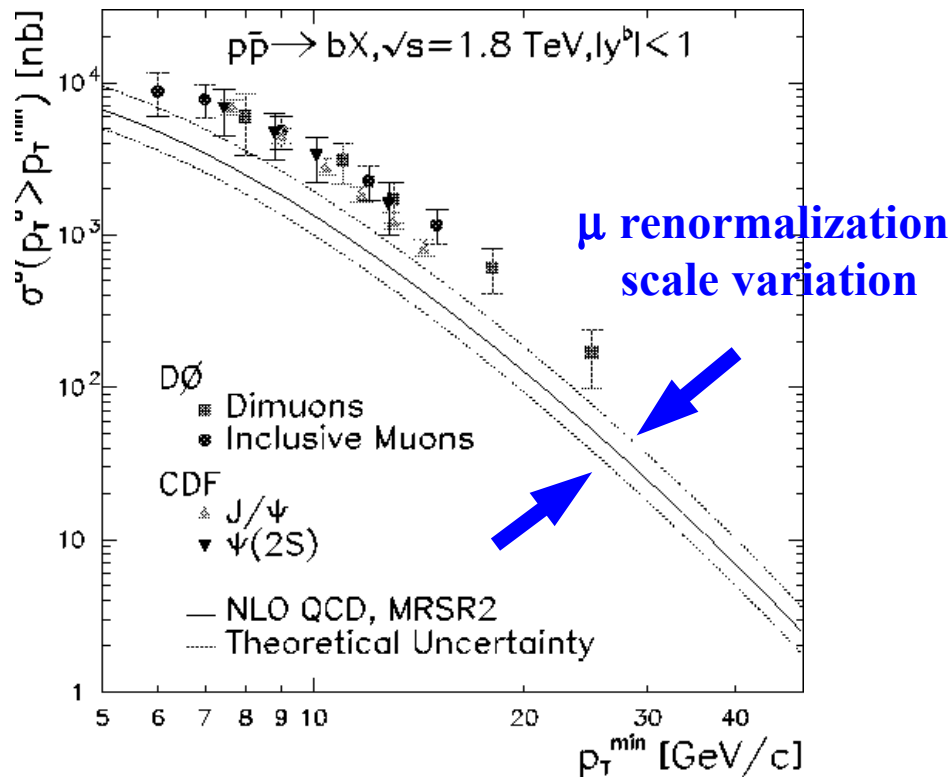
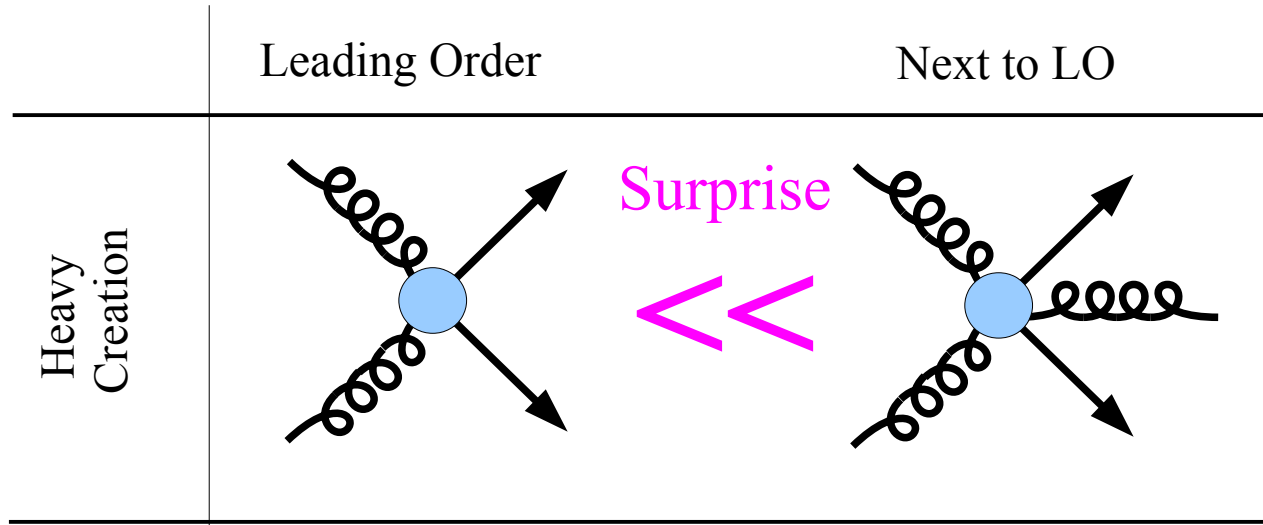


Fixed-Flavor Scheme



Variable-Flavor Scheme

NLO Fixed-Flavor Scheme

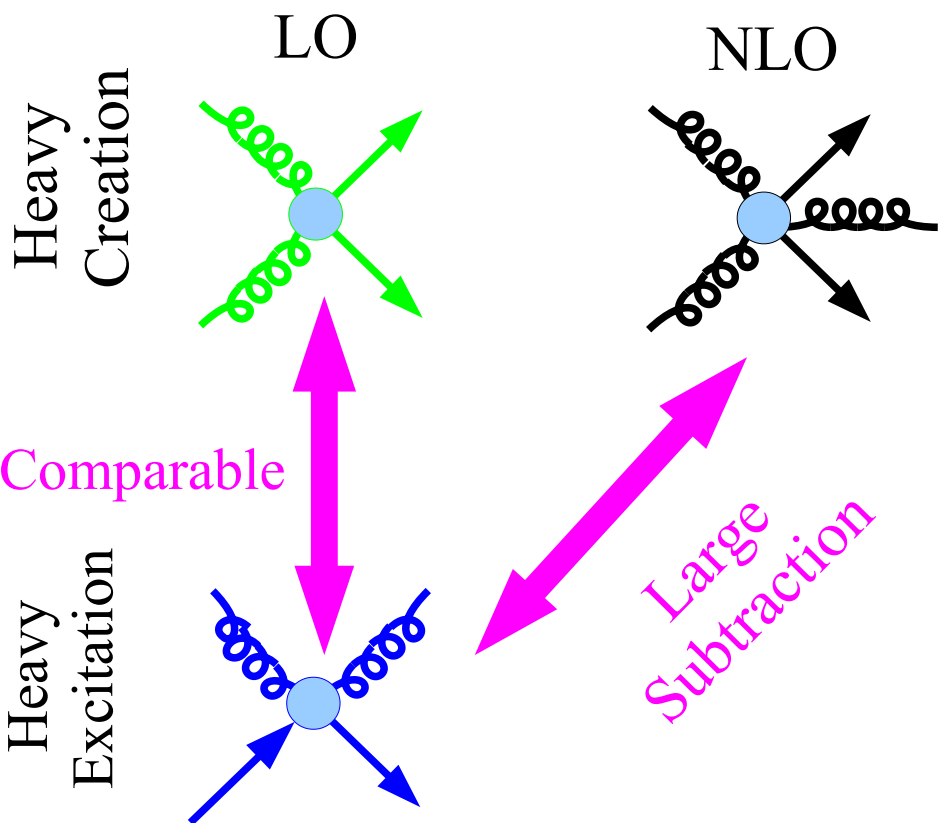


Surprise: NLO / LO ~ 2

But, theory still below data

Nason, Dawson, Ellis
 Beenakker, Kuijf, Van Neerven, Smith

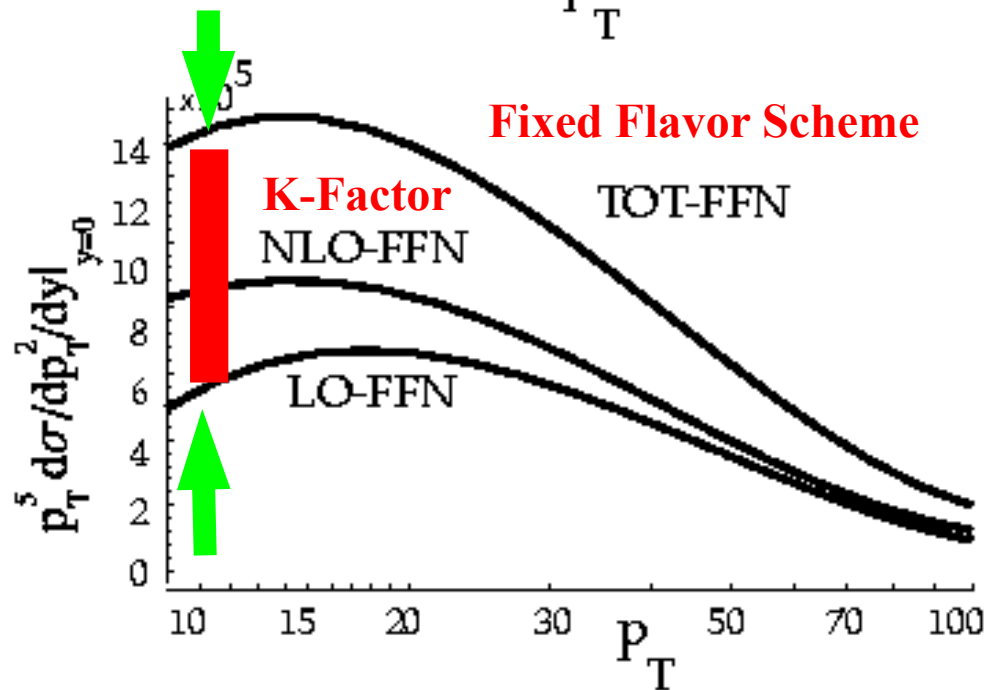
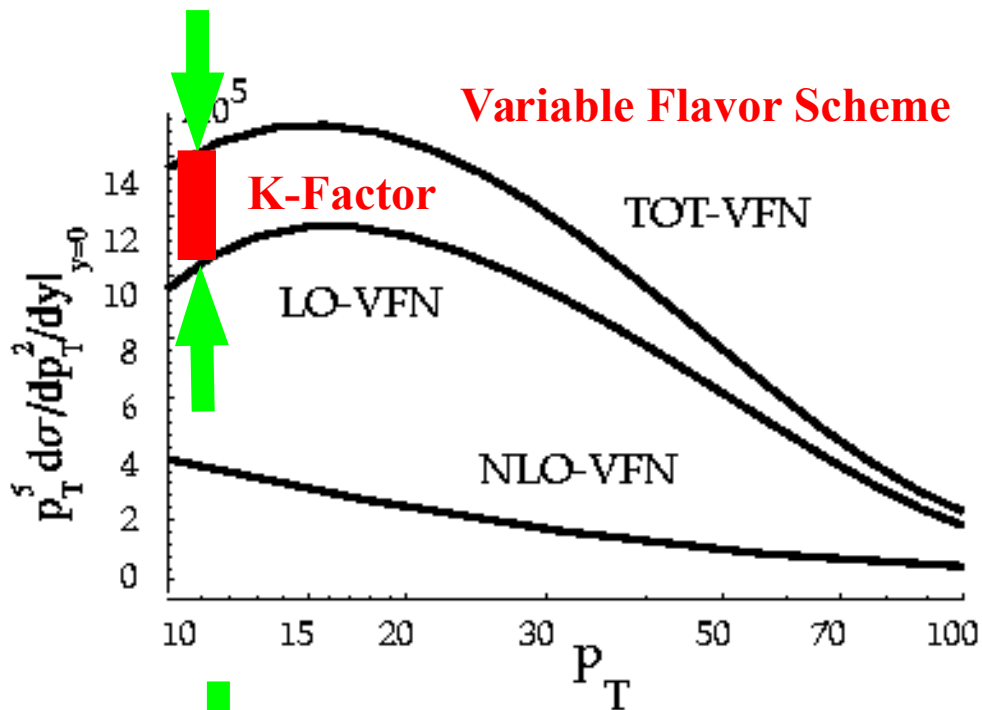
NLO Variable Flavor Scheme



Net result:

- Reduction of μ -dependence
- 30% to 50% increase in σ

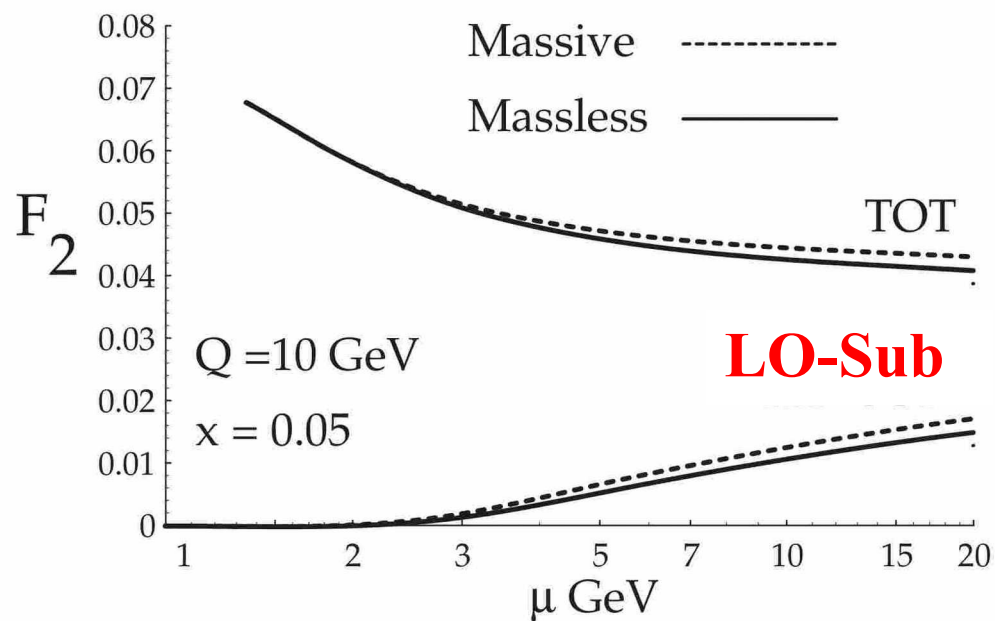
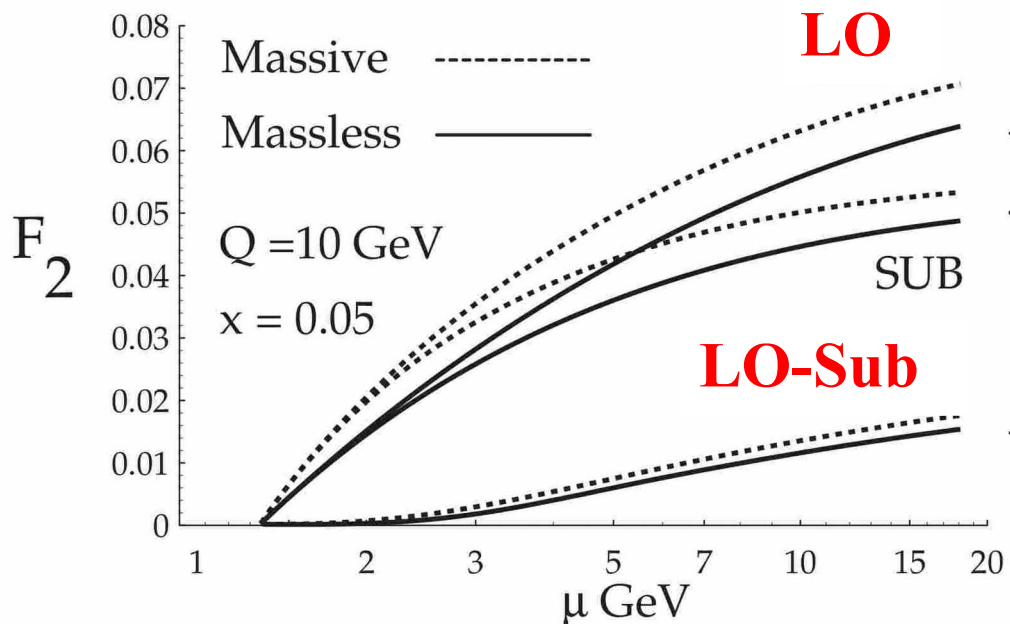
Aivazis, Collins, Olness, Tung
Olness, Scalise, Tung



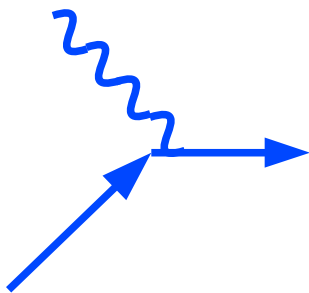
Mass- Independent Evolution.

Why is it valid?

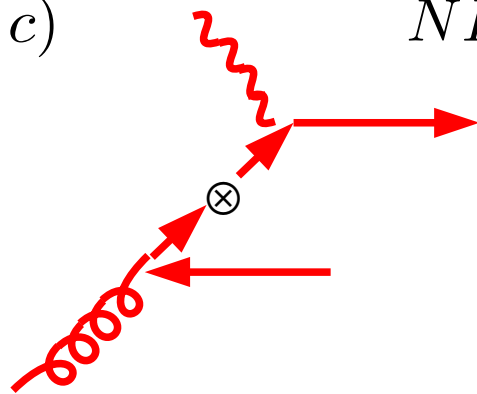
Effect of Heavy Quark Mass in the Calculation is Trivial



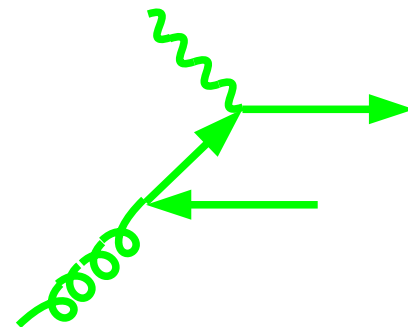
$$LO = \int f(P \rightarrow a) \otimes \sigma(a \rightarrow c)$$



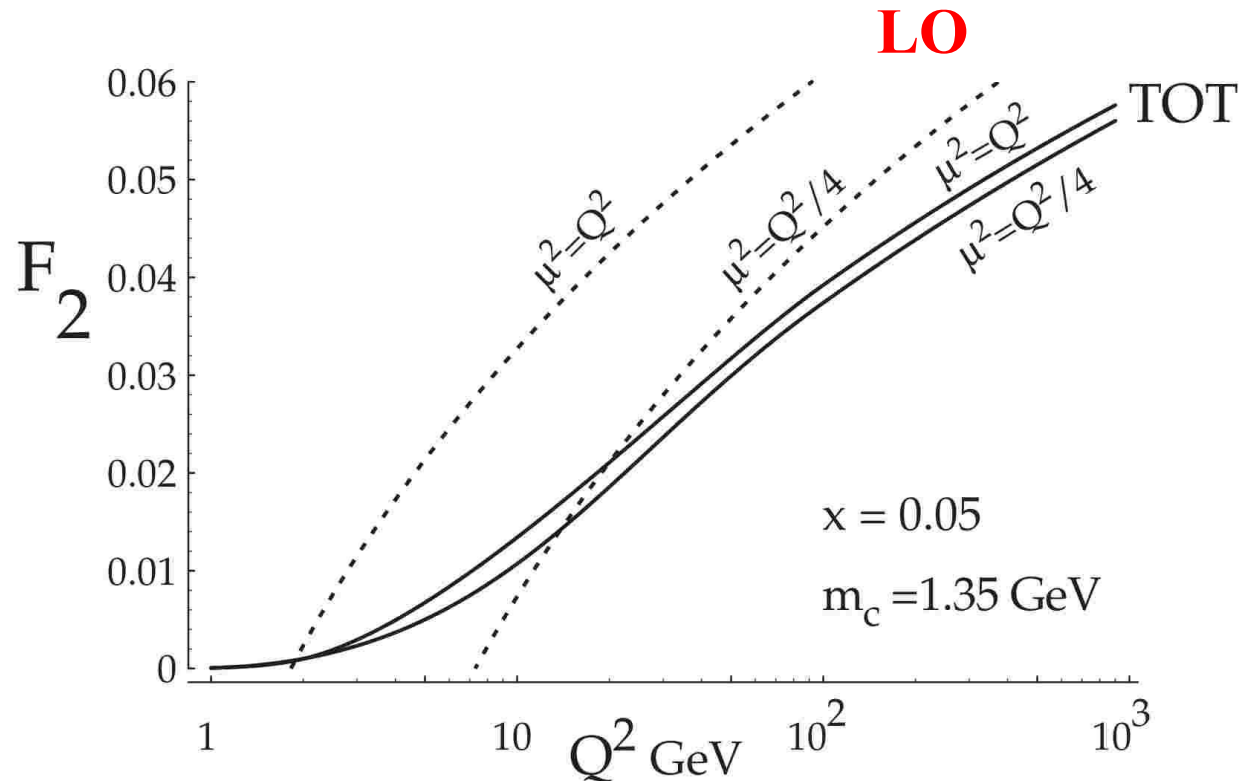
$$NLO = \int f(P \rightarrow g) \otimes \sigma(g \rightarrow c)$$



$$SUB = \int f(P \rightarrow g) \otimes {}^1P(g \rightarrow a) \otimes \sigma(a \rightarrow c)$$



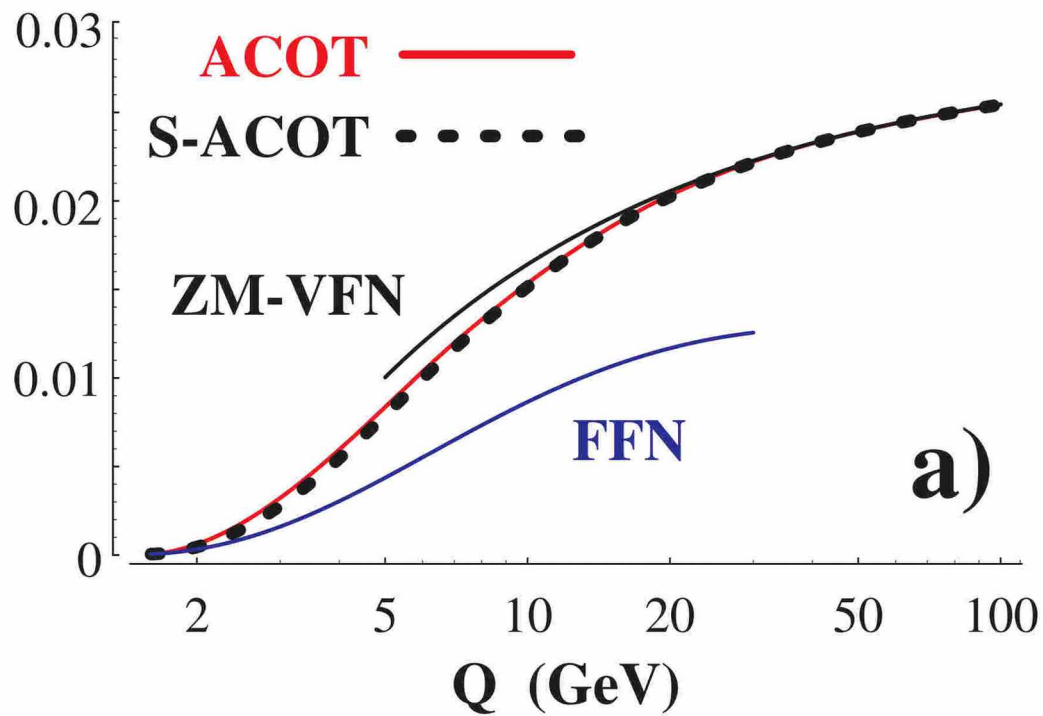
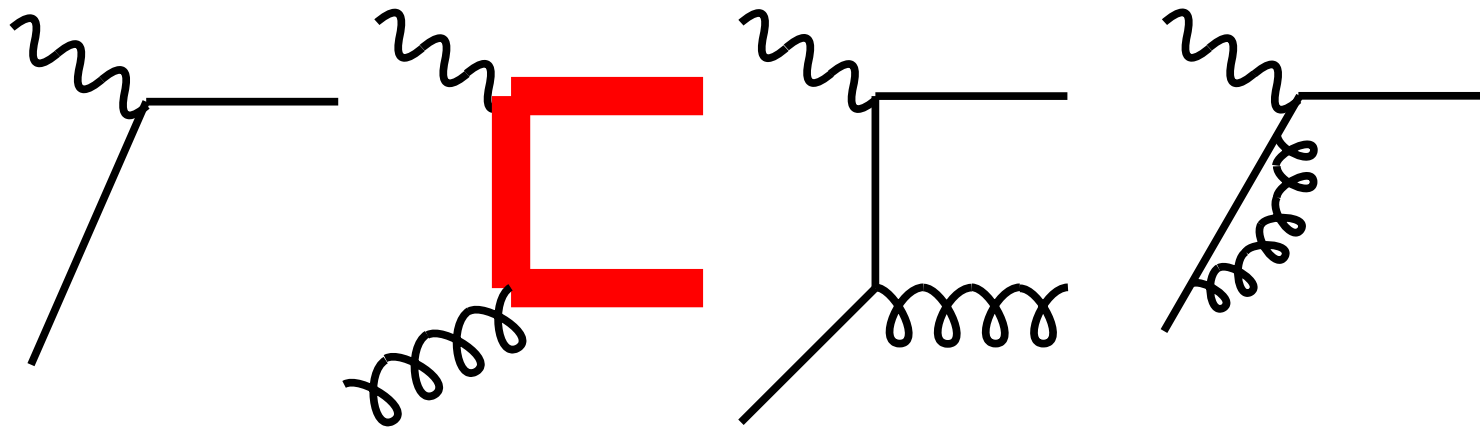
Variation of σ vs. renormalization scale μ



LO = HE result is very sensitive to the choice of scale (i.e., $\mu^2=Q^2$ or $Q^2/4$)
TOT result (higher order) is stable **w.r.t.** the choice of scale

An accurate calculation must be stable
as the renormalization scale varies

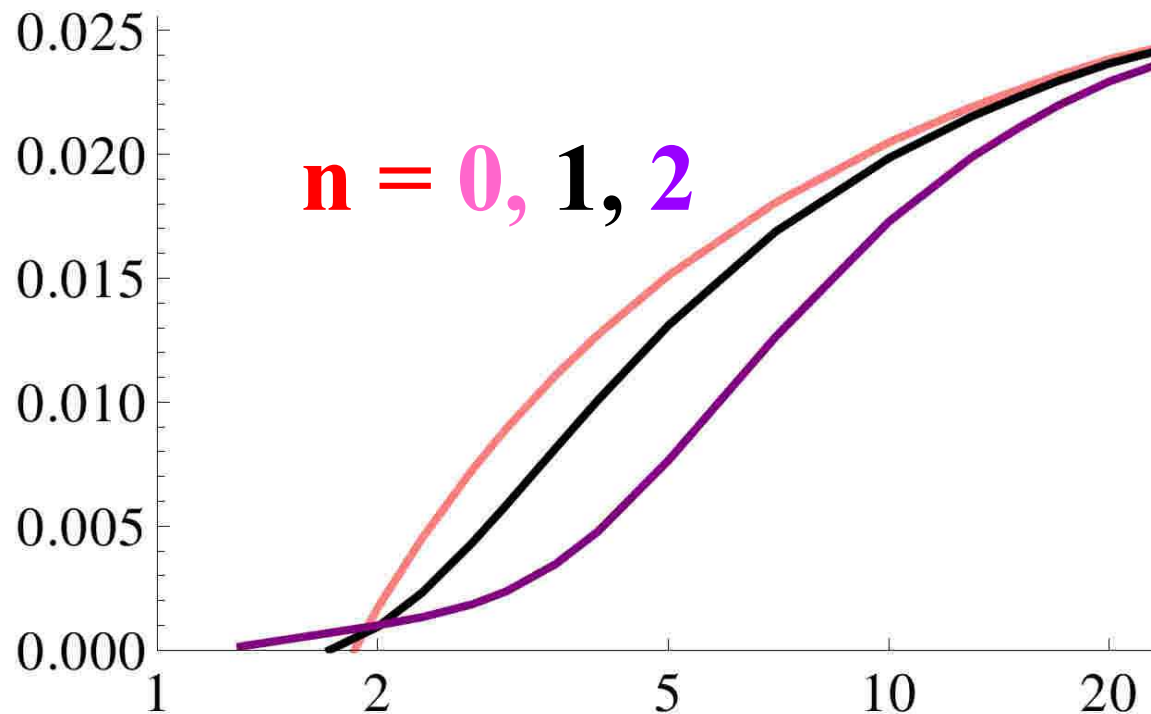
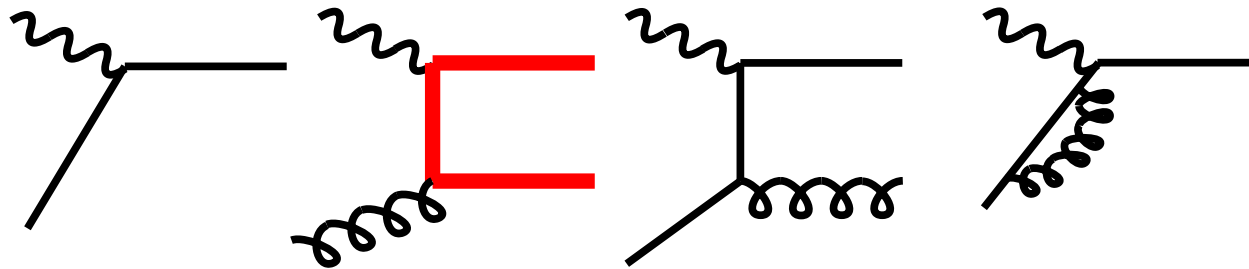
Simplified ACOT



χ -Prescription

rescaling:

$$x \rightarrow \chi = x \left[1 + \frac{(nm)^2}{Q^2} \right]$$



Higher Orders

An example...

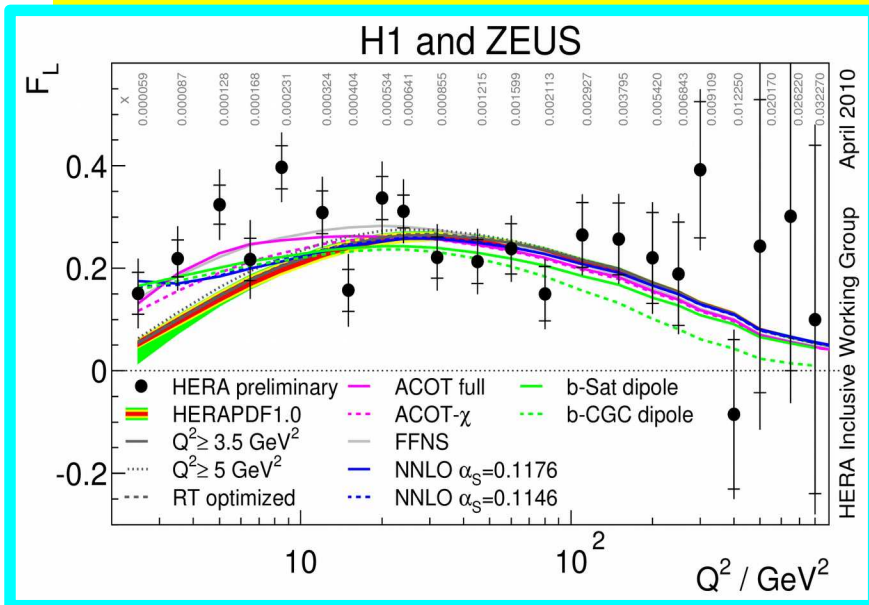
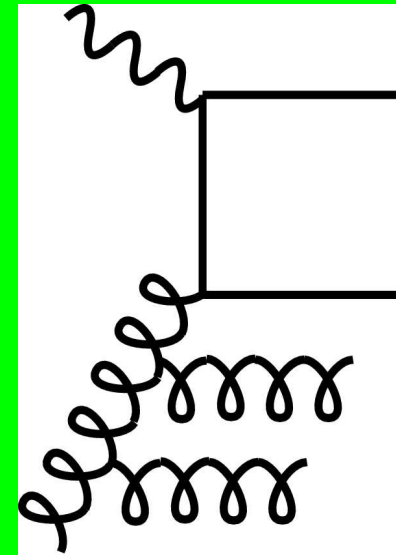
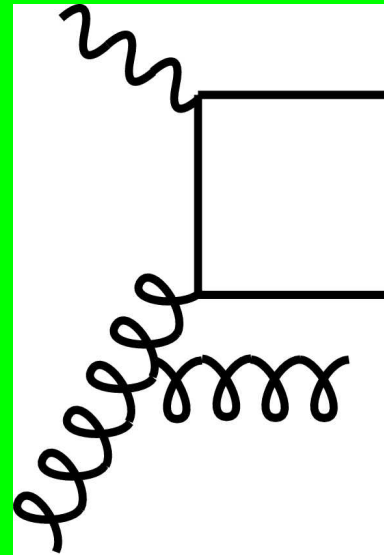
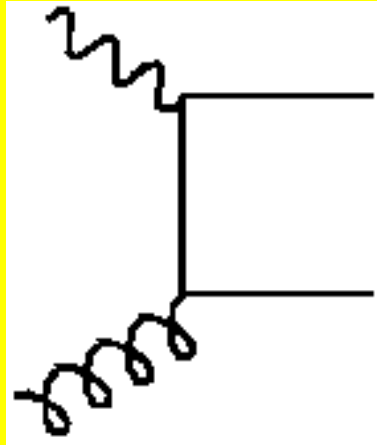
ACOT@ NNLO + N³LO

LO

NLO

N2LO

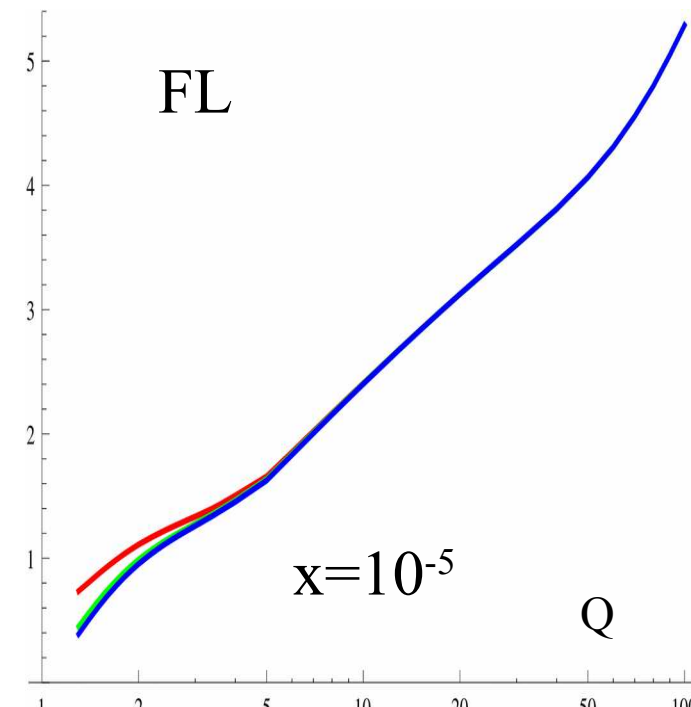
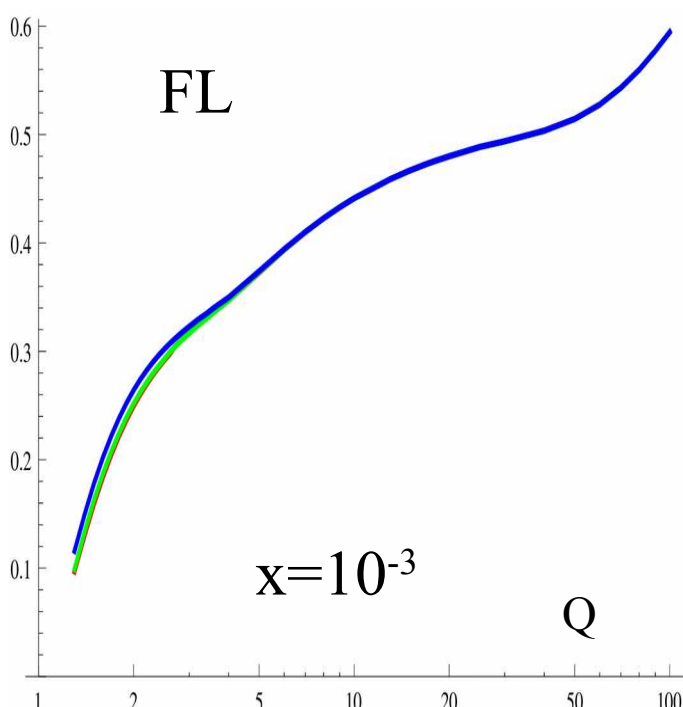
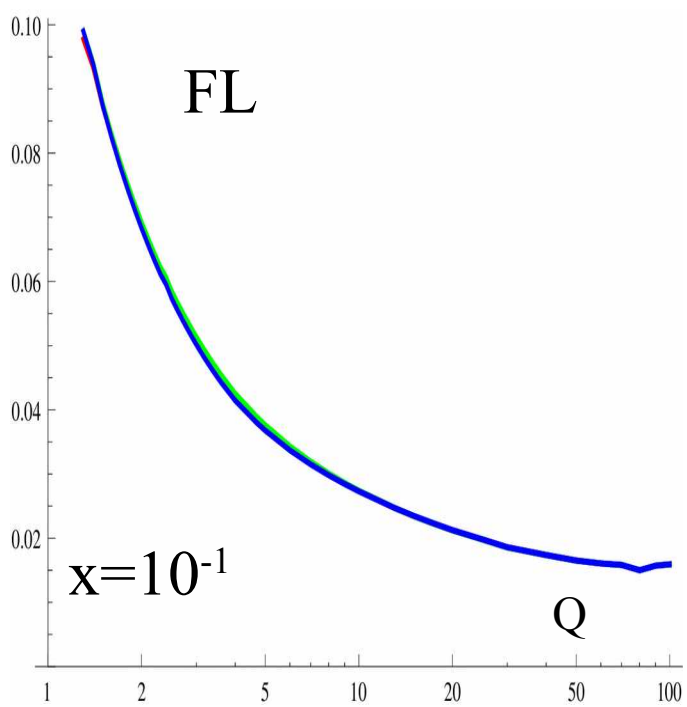
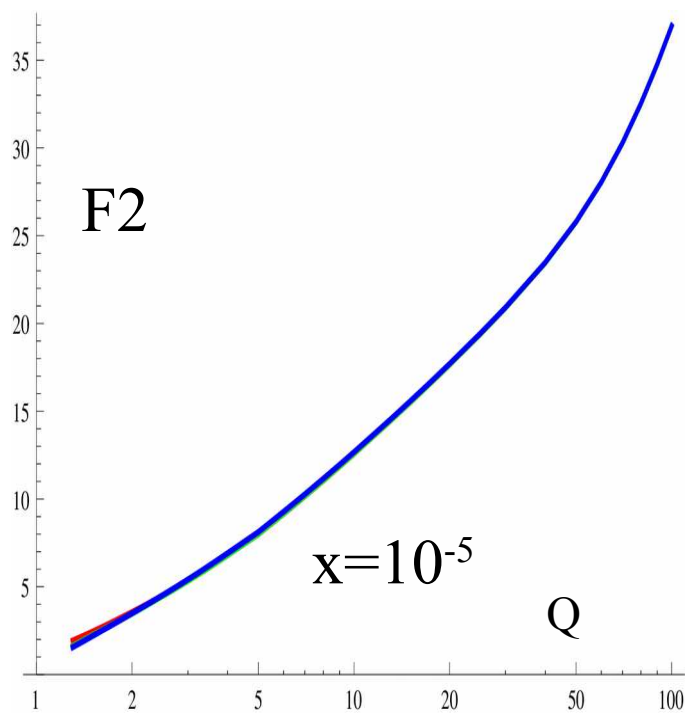
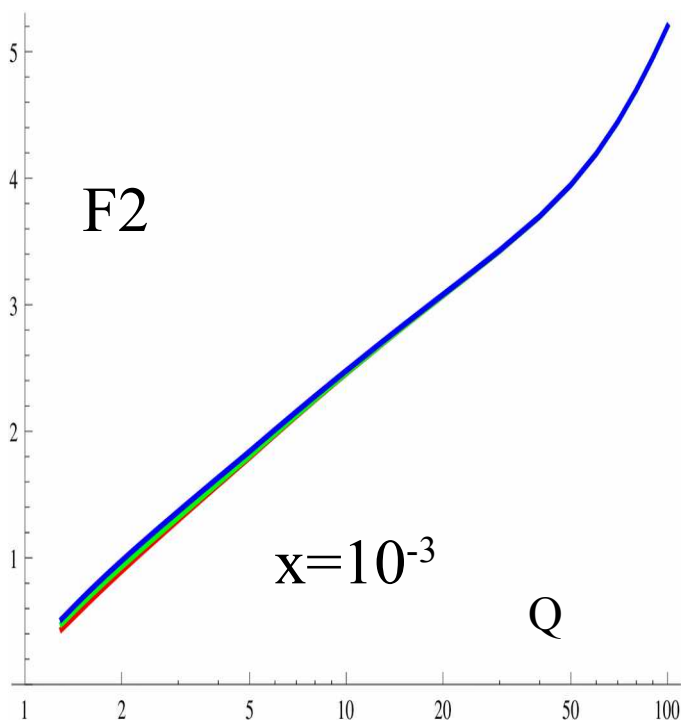
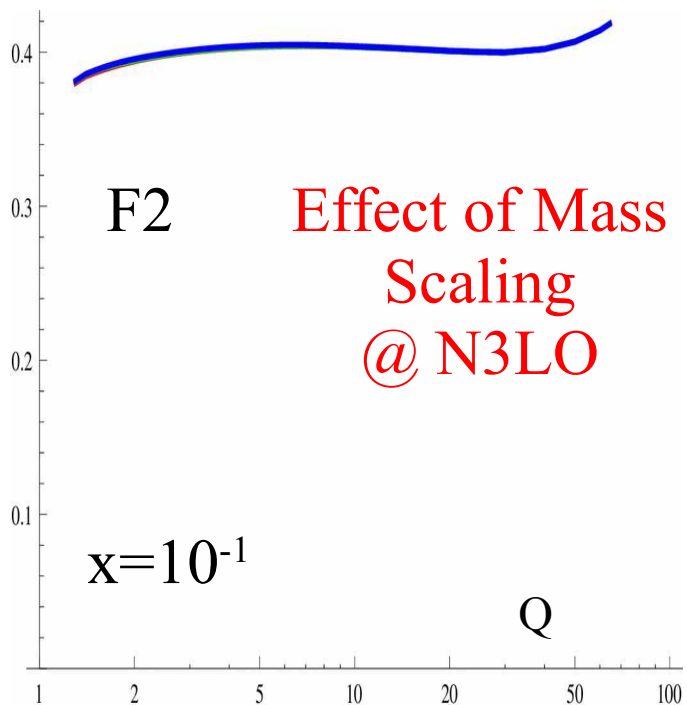
N3LO

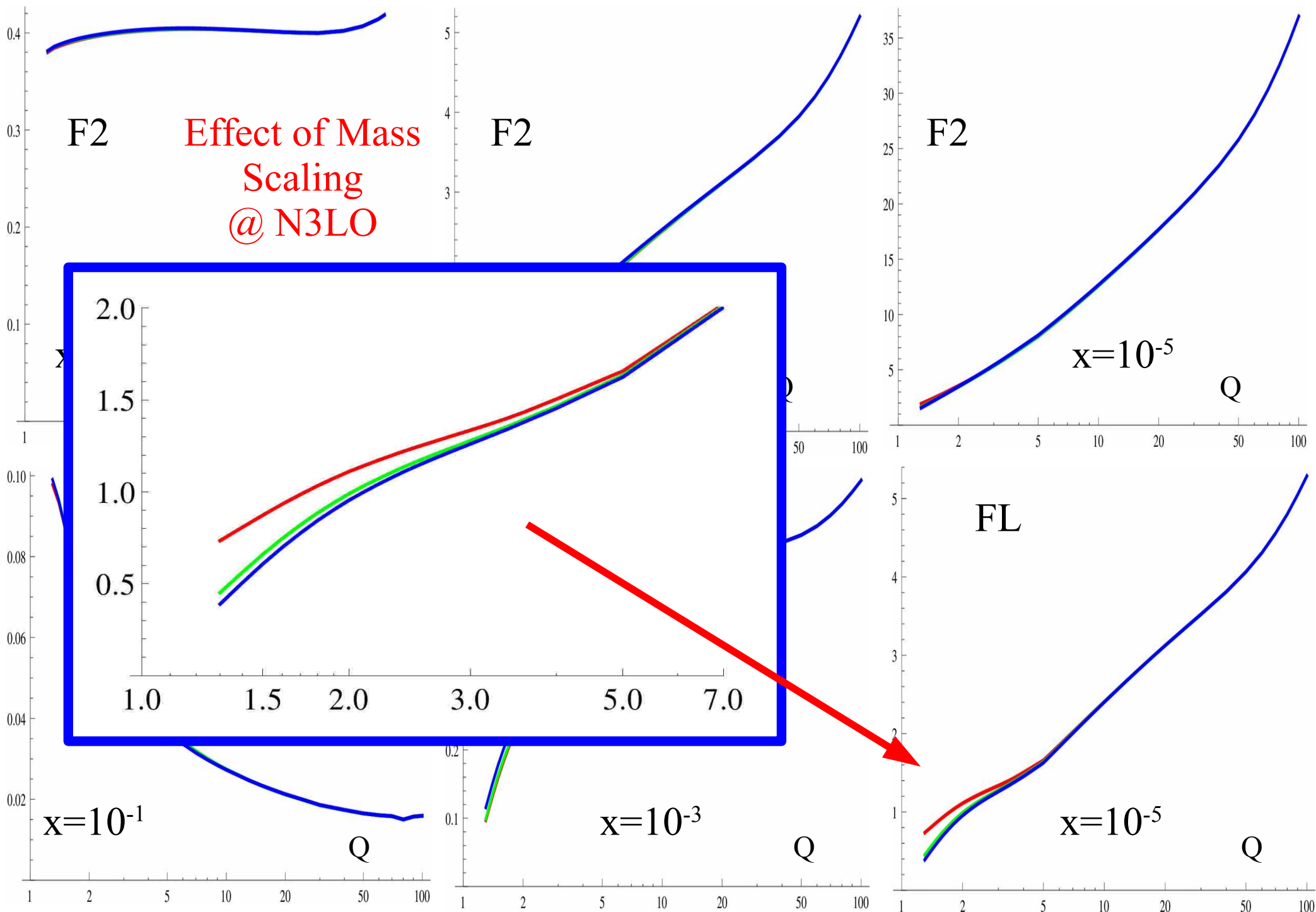


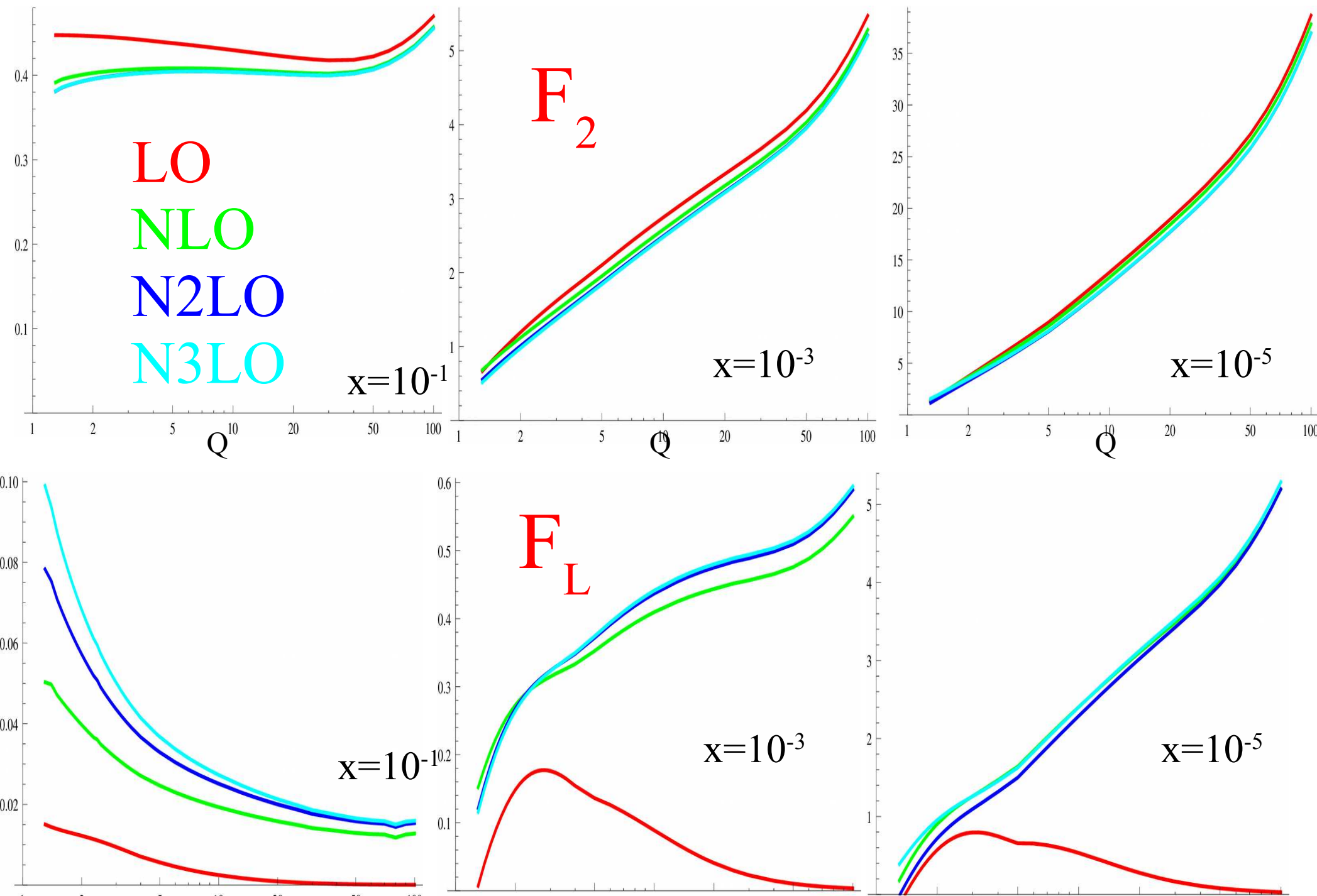
Masses are important

Higher Orders are important

$$F_L \sim \frac{m^2}{Q^2} q(x) + \alpha_S \{c_g \otimes g(x) + c_q \otimes q(x)\}$$





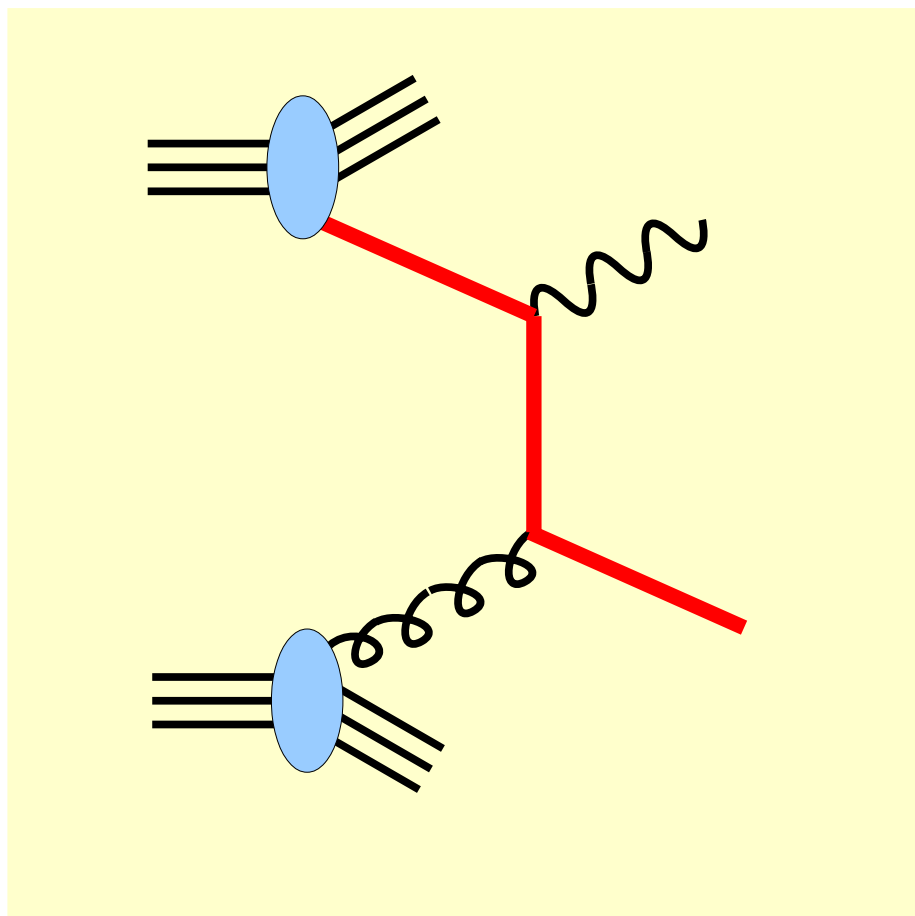


... what about the

Heavy Quarks

at high energies

Tevatron & LHC

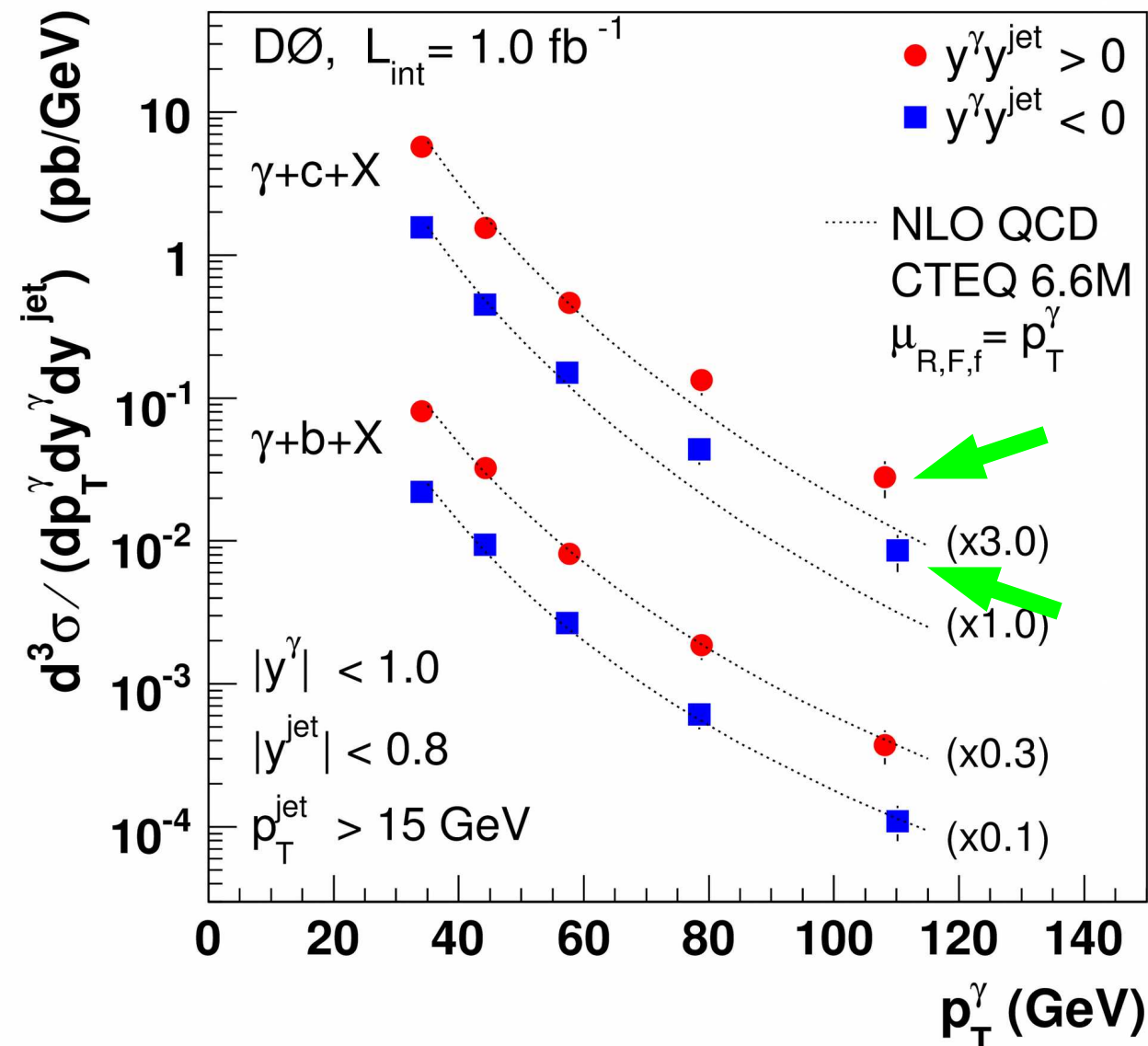


$$c \ g \rightarrow c \ \gamma$$

$$b \ g \rightarrow b \ \gamma$$

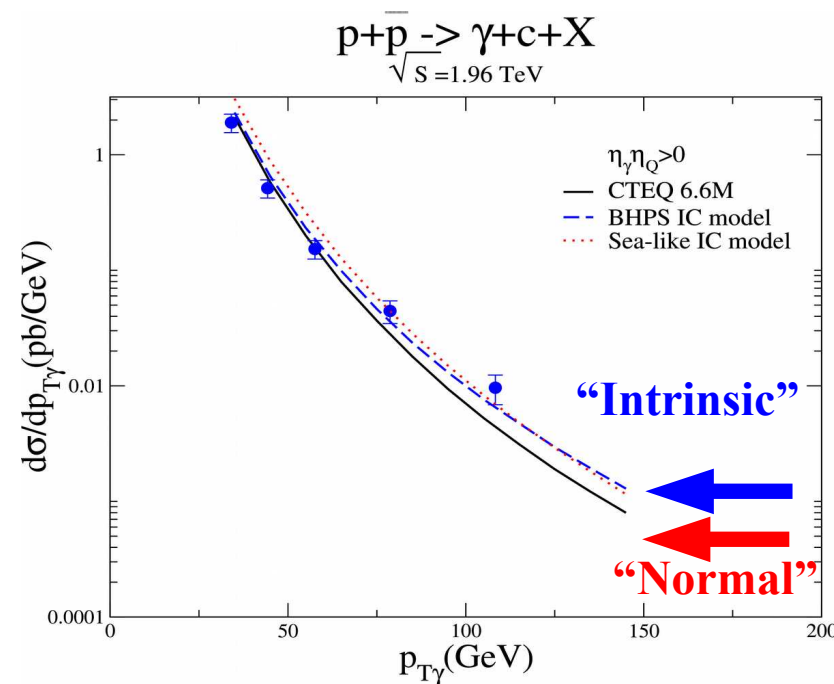
$$s \ g \rightarrow c \ W$$

$$c \ g \rightarrow b \ W$$



Excess in Charm,
NOT Bottom

only at high PT



DGLAP Evolution equations ...

including **ordinary** Q_0 and **intrinsic** Q_1 heavy quark

$$\begin{aligned} \dot{g} &= P_{gg} \otimes g + P_{gq} \otimes q + P_{gQ} \otimes Q_0 + \cancel{P_{gQ} \otimes Q_1}, \\ \dot{q} &= P_{qg} \otimes g + P_{qq} \otimes q + P_{qQ} \otimes Q_0 + \cancel{P_{qQ} \otimes Q_1}, \\ \dot{Q}_0 + \dot{Q}_1 &= P_{Qg} \otimes g + P_{Qq} \otimes q + P_{QQ} \otimes Q_0 + P_{QQ} \otimes Q_1. \end{aligned}$$

neglect

Equations decouple:

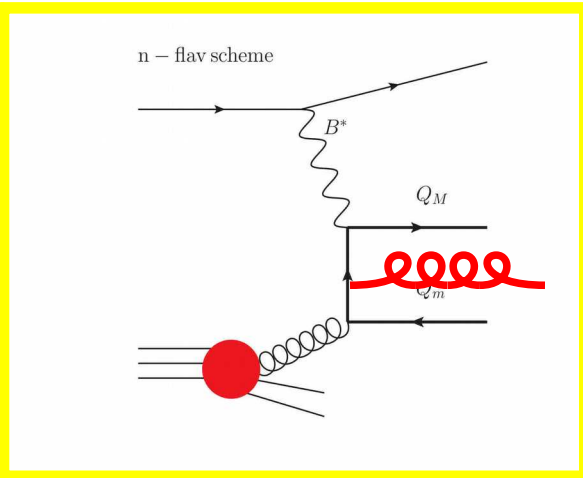
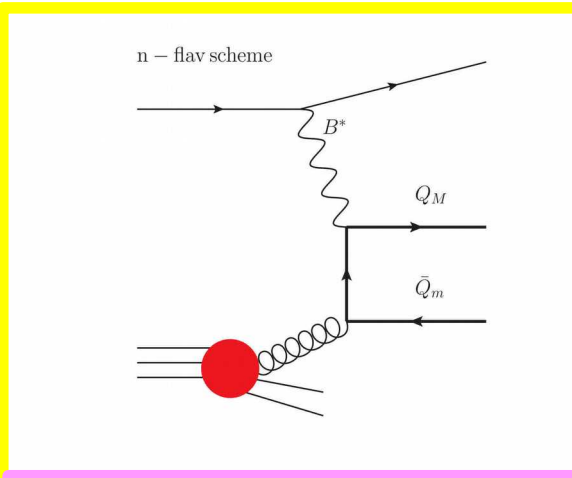
Intrinsic component evolves independently
 Scale set by m_Q
 Adjust normalization by simple rescaling

$$\dot{Q}_1 = P_{QQ} \otimes Q_1.$$

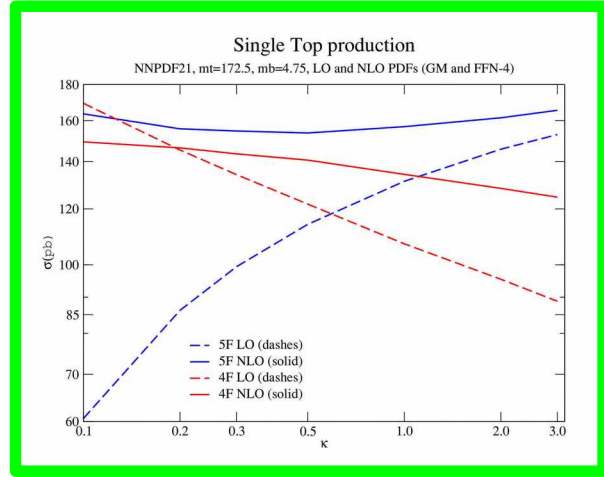
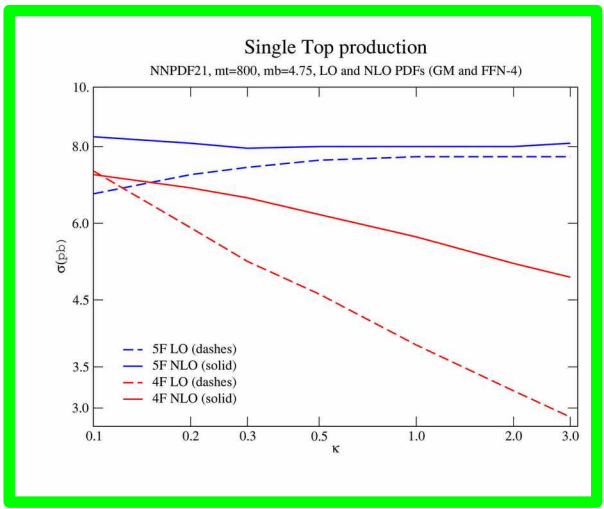
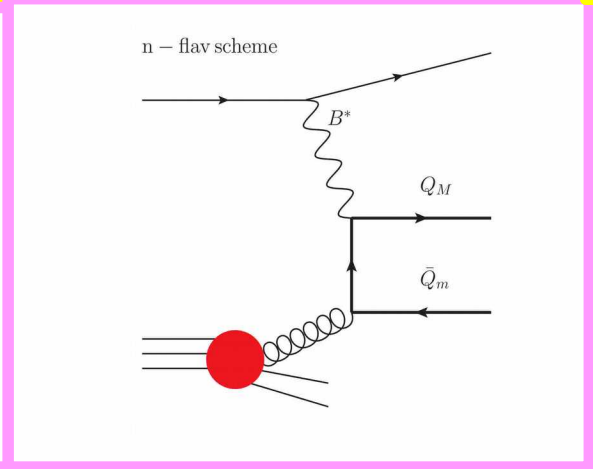
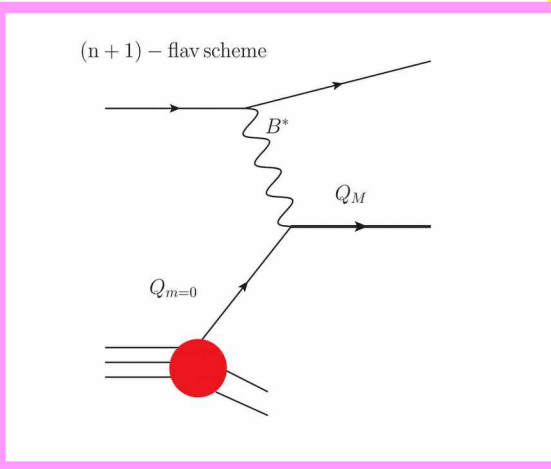
$$c_1(x) = \bar{c}_1(x) \propto x^2 [6x(1+x) \ln x + (1-x)(1+10x+x^2)]$$

Thoughts

4 Flavor NLO



5 Flavor NLO



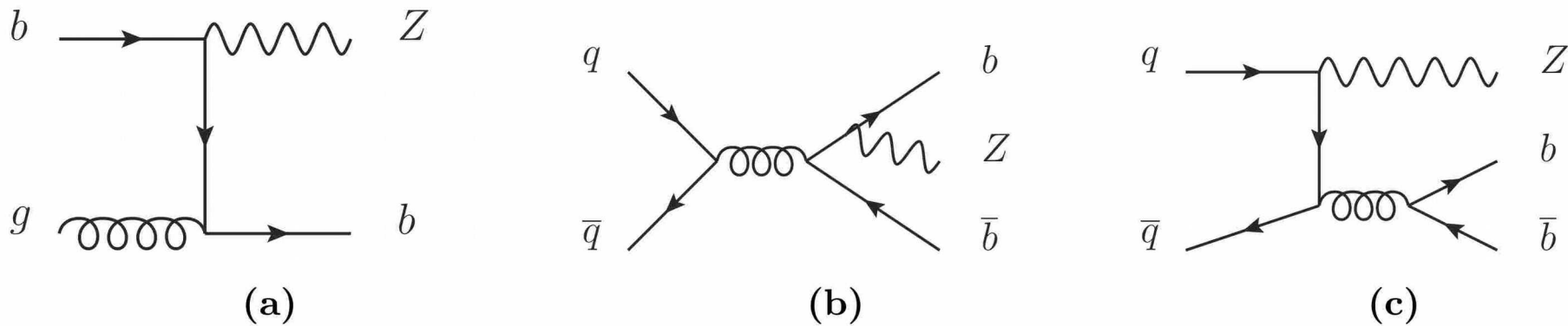
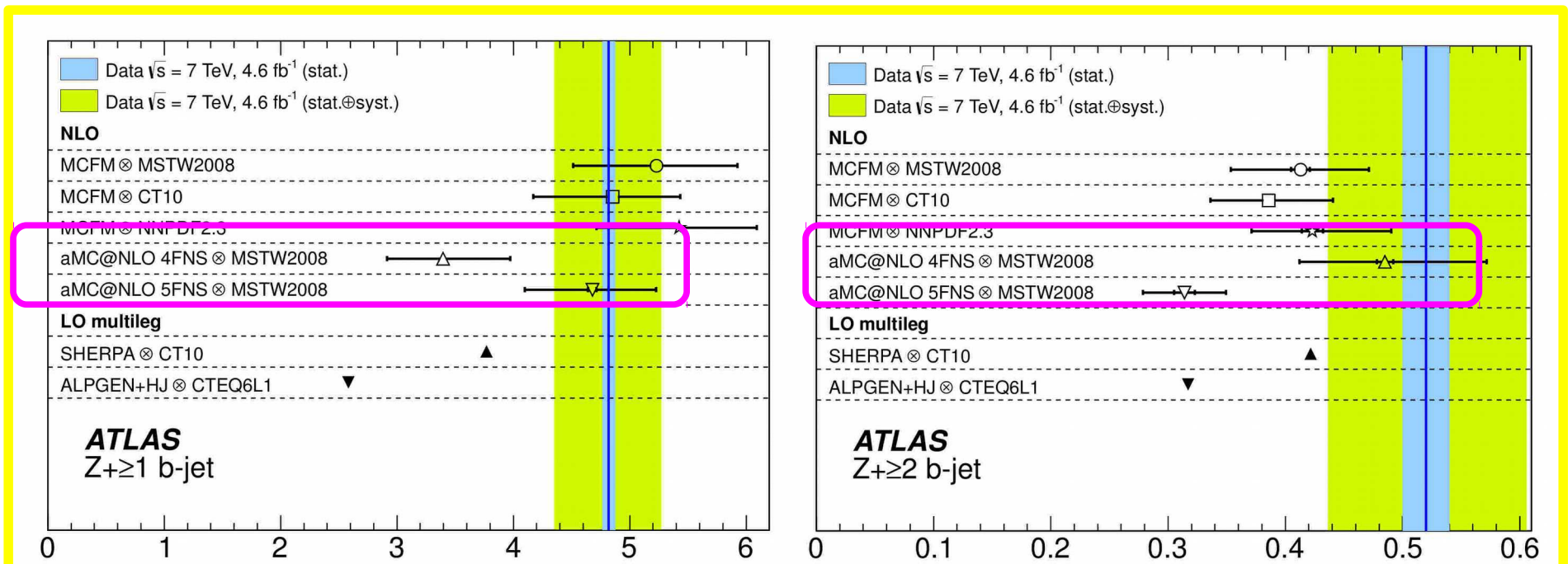
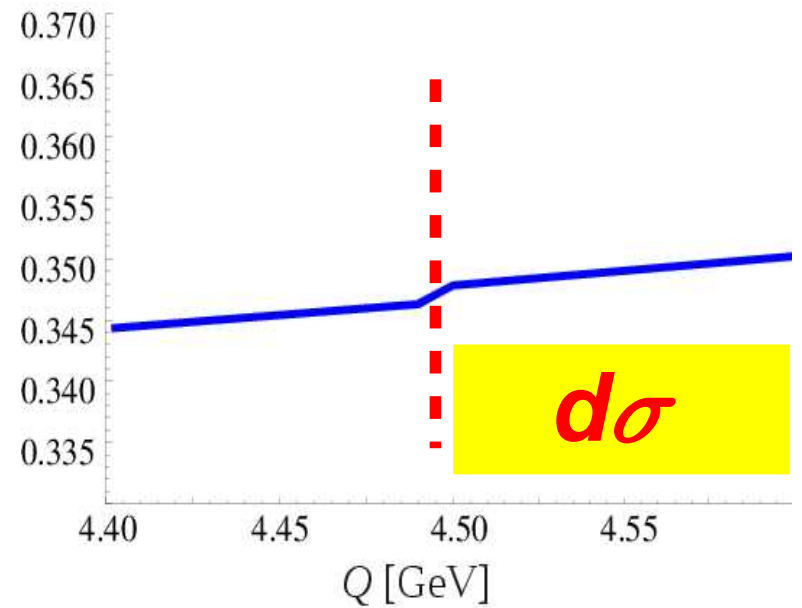
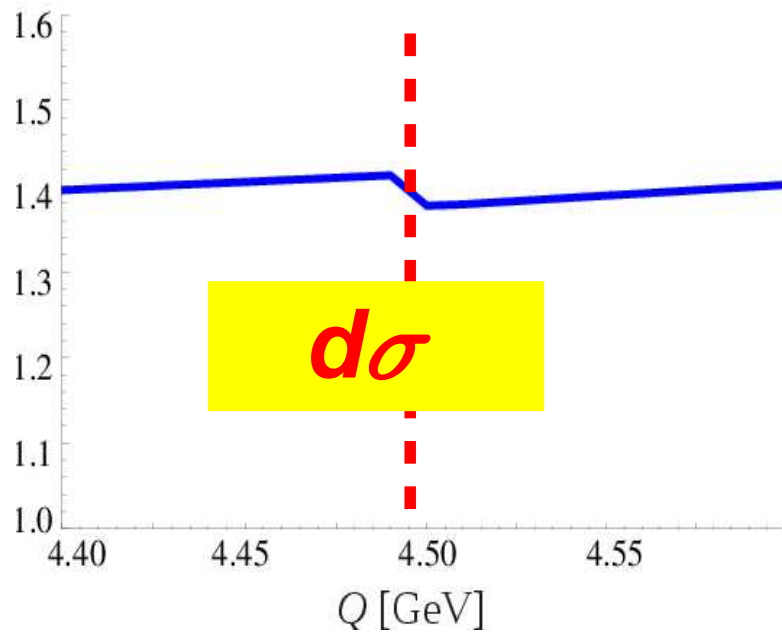
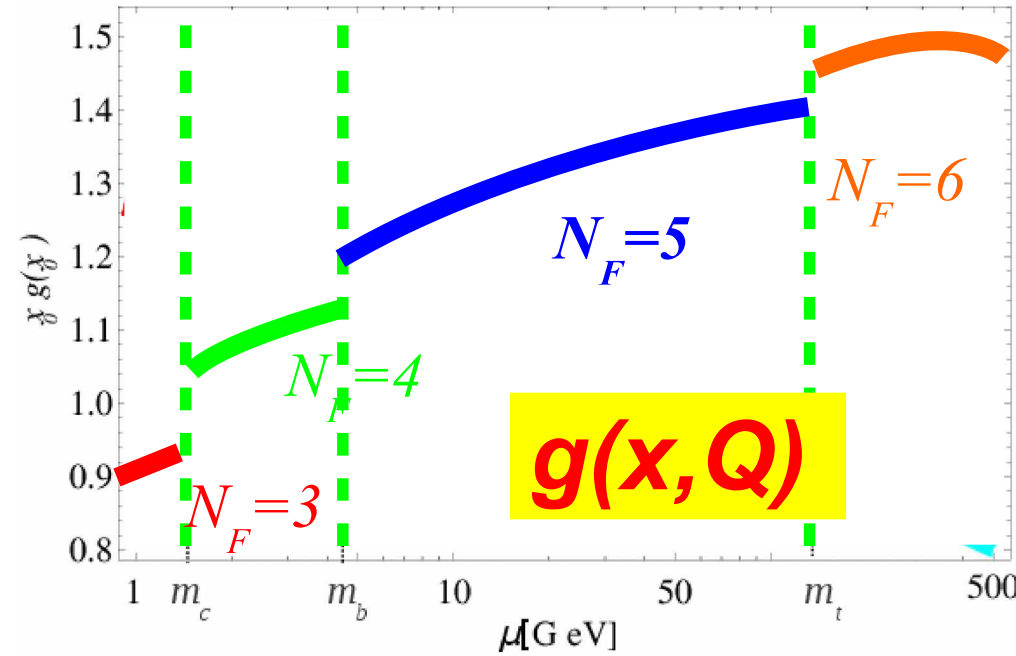
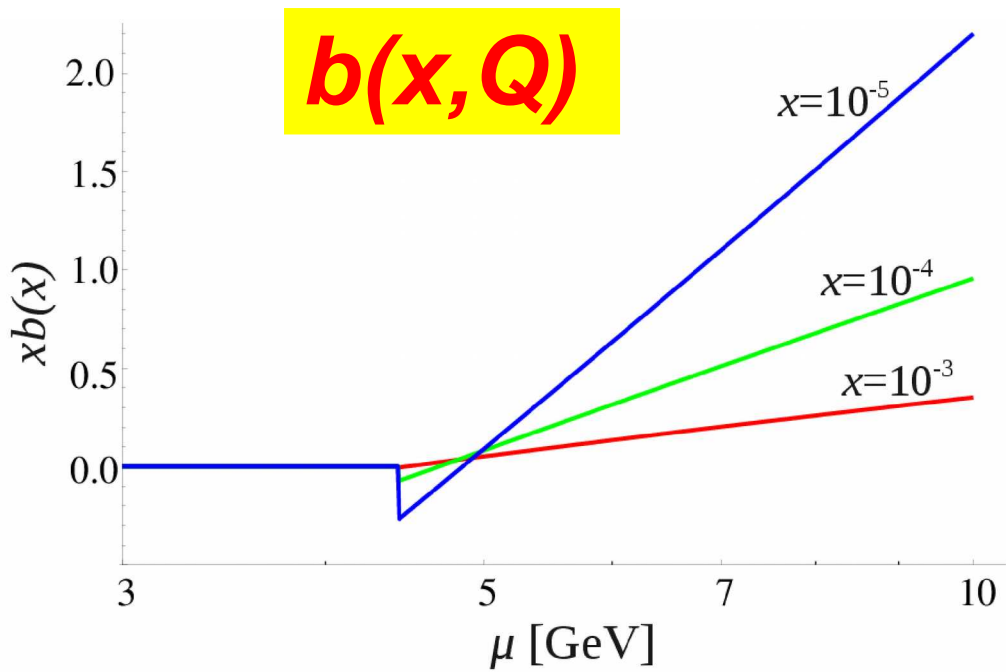


Figure 1. Leading order Feynman diagrams contributing to $Z+b$ -jets production. Process 1a is only present in a 5FNS calculation, while 1b and 1c are present in both the 4FNS and 5FNS calculations.

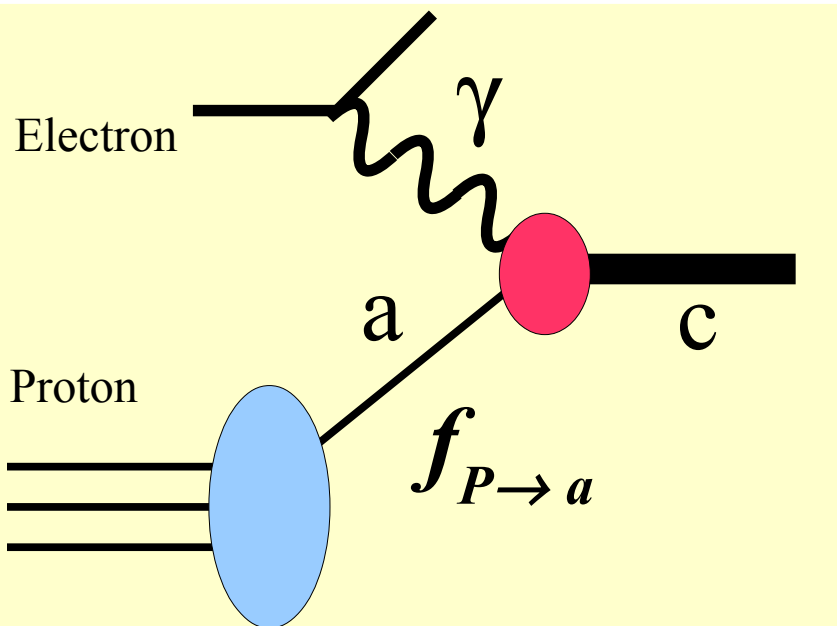
- * ACOT (& variations) allow full mass dependence
 - based on CWZ renormalization scheme
 - systematically applied to all orders
- * Massless Evolution ($\overline{\text{MS}}$): no loss of information
- * S-ACOT: can eliminate SOME masses WITHOUT loss of information
- * χ -prescription: rescaling: $x \rightarrow \chi = x(1+n m^2/Q^2)$
 - ... helps at threshold; ALTERNATE: turn on at $2m$ or $4m$, ...
 - ... use rescaling to estimate higher order contributions: N2LO, N3LO
- * 5-Flavor Scheme encompasses 4-Flavor Scheme
 - ... beware how higher-orders are “counted”
 - ... requires care when “truncated”: e.g. $Z+b$ vs $Z+bb$

Lots of progress, in part due to xFitter. We'll need it for Precisions LHC

Leftover



Pictorial Demonstration of Scheme Consistency

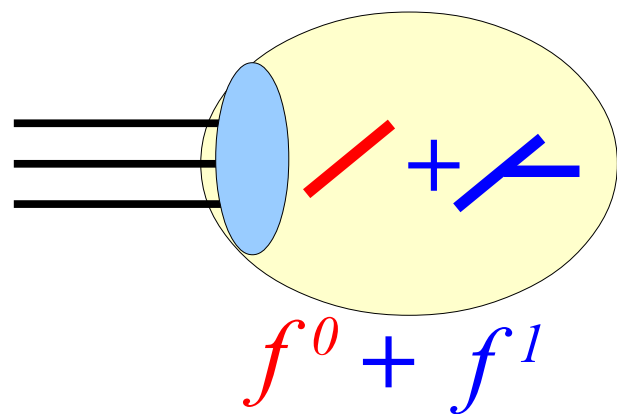


Parton Model

$$\sigma(Q^2) = f(\mu, \alpha_s) \otimes \hat{\omega}(Q^2, \mu^2, \alpha_s)$$

Evolution Equation

$$\frac{df}{\ln[\mu^2]} = P \otimes f$$

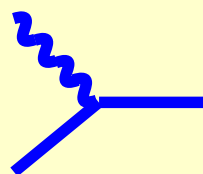


LO

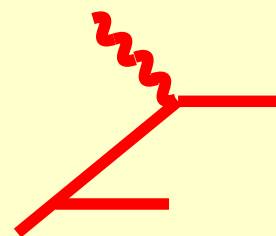
NLO

SUB

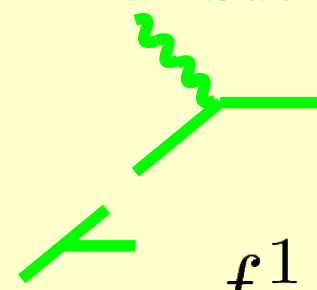
Subtraction



+



-



σ_0

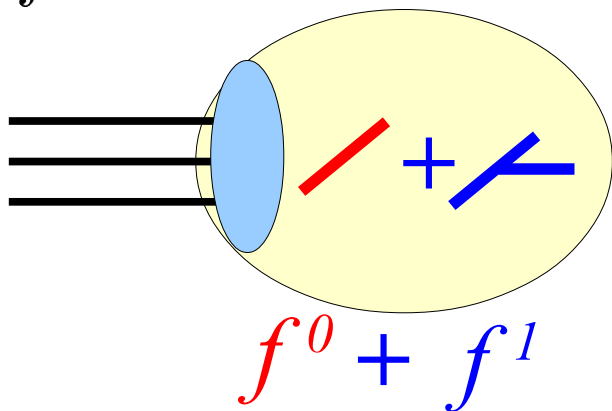
σ_1

$f^1 \otimes \sigma_0$

$f^0 + f^1$

Pictorial Demonstration of Scheme Consistency

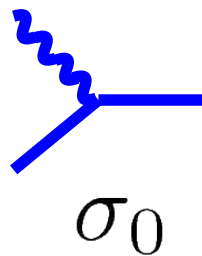
$$f^0 \equiv \delta$$



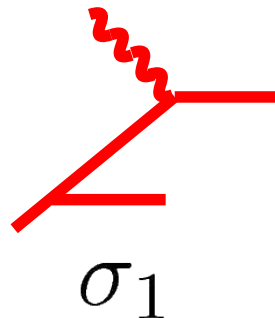
LO

NLO

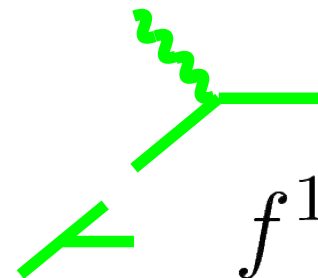
SUB
Subtraction



+



-



$\otimes \sigma_0$

Complete NLO Term

$$[\delta + f^1] \otimes [\sigma_0 + \sigma_1 - f^1 \otimes \sigma_0]$$

$$f^1 \sim \frac{\alpha_s}{2\pi} P^{(1)}$$

*P⁽¹⁾ defined by
scheme choice*

$\sigma_0 + \sigma_1 + f^1 \otimes \sigma_0 - f^1 \otimes \sigma_0 + \mathcal{O}(\alpha_s^2)$

Contains BOTH collinear and non-collinear region
 From PDF Evolution
 From NLO Subtraction

*QCD is
Bullet-proof*

Multi-Scale Problems are Challenging

Two-Loop Total Cross Section: One Scale

$$\sigma(Q^2) = \sigma_0 \left\{ 1 + \frac{\alpha_s(Q^2)}{4\pi} (3C_F) + \left[\frac{\alpha_s(Q^2)}{4\pi} \right]^2 \left[-C_F^2 \left[\frac{3}{2} \right] + C_F C_A \left[\frac{123}{2} - 44\zeta(3) \right] + C_F T n_f (-22 + 16\zeta(3)) \right] \right\}$$

Two-Loop Drell-Yan Cross Section: Two Scales

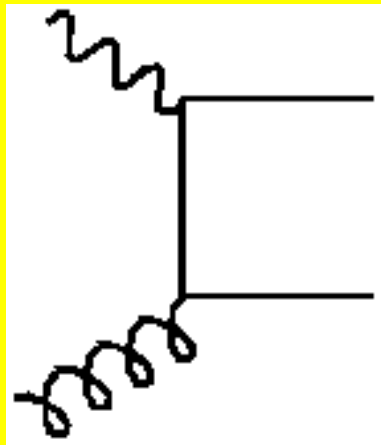
$$\begin{aligned} H_{q\bar{q}}^{(2),S+V}(z) = & \left[\frac{\alpha_s}{4\pi} \right]^2 \delta(1-z) \left\{ C_A C_F \left[\left[\frac{193}{3} - 24\zeta(3) \right] \ln \left[\frac{Q^2}{M^2} \right] - 11 \ln^2 \left[\frac{Q^2}{M^2} \right] - \frac{12}{5} \zeta(2)^2 + \frac{592}{9} \zeta(2) + 28\zeta(3) - \frac{1535}{12} \right] \right. \\ & + C_F^2 \left[\left[18 - 32\zeta(2) \right] \ln^2 \left[\frac{Q^2}{M^2} \right] + \left[24\zeta(2) + 176\zeta(3) - 93 \right] \ln \left[\frac{Q^2}{M^2} \right] \right. \\ & \left. \left. + \frac{8}{5} \zeta(2)^2 - 70\zeta(2) - 60\zeta(3) + \frac{511}{4} \right] \right. \\ & \left. + n_f C_F \left[2 \ln^2 \left[\frac{Q^2}{M^2} \right] - \frac{34}{3} \ln \left[\frac{Q^2}{M^2} \right] + 8\zeta(3) - \frac{112}{9} \zeta(2) + \frac{127}{6} \right] \right\} \\ & + C_A C_F \left[-\frac{44}{3} \mathcal{D}_0(z) \ln^2 \left[\frac{Q^2}{M^2} \right] + \left\{ \left[\frac{536}{9} - 16\zeta(2) \right] \mathcal{D}_0(z) - \frac{176}{3} \mathcal{D}_1(z) \right\} \ln \left[\frac{Q^2}{M^2} \right] \right. \\ & \left. - \frac{176}{3} \mathcal{D}_2(z) + \left[\frac{1072}{9} - 32\zeta(2) \right] \mathcal{D}_1(z) + \left[56\zeta(3) + \frac{176}{3} \zeta(2) - \frac{1616}{27} \right] \mathcal{D}_0(z) \right] \\ & + C_F^2 \left[\left[64\mathcal{D}_1(z) + 48\mathcal{D}_0(z) \right] \ln^2 \left[\frac{Q^2}{M^2} \right] + \left\{ 192\mathcal{D}_2(z) + 96\mathcal{D}_1(z) - \left[128 + 64\zeta(2) \right] \mathcal{D}_0(z) \right\} \ln \left[\frac{Q^2}{M^2} \right] \right. \\ & \left. + 128\mathcal{D}_3(z) - \left(128\zeta(2) + 256 \right) \mathcal{D}_1(z) + 256\zeta(3) \mathcal{D}_0(z) \right] \\ & + n_f C_F \left[\frac{8}{3} \mathcal{D}_0(z) \ln^2 \left[\frac{Q^2}{M^2} \right] + \left[\frac{32}{3} \mathcal{D}_1(z) - \frac{80}{9} \mathcal{D}_0(z) \right] \ln \left[\frac{Q^2}{M^2} \right] + \frac{32}{3} \mathcal{D}_2(z) - \frac{160}{9} \mathcal{D}_1(z) + \left[\frac{224}{27} - \frac{32}{3} \zeta(2) \right] \mathcal{D}_0(z) \right] . \end{aligned}$$

Ref:
CTEQ
Handboo
k

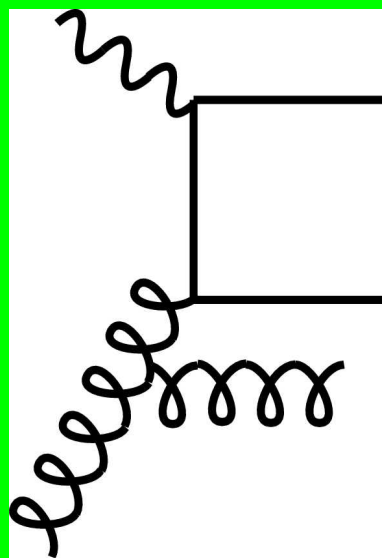
LO



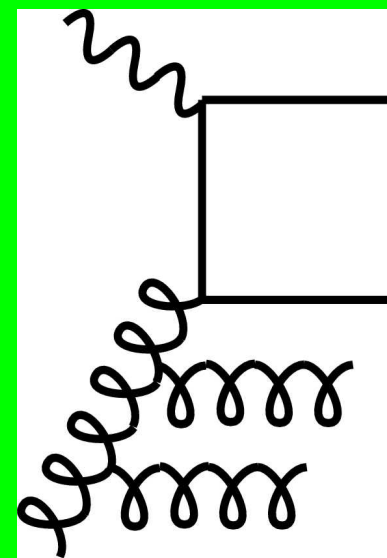
NLO



N2LO



N3LO



Full ACOT

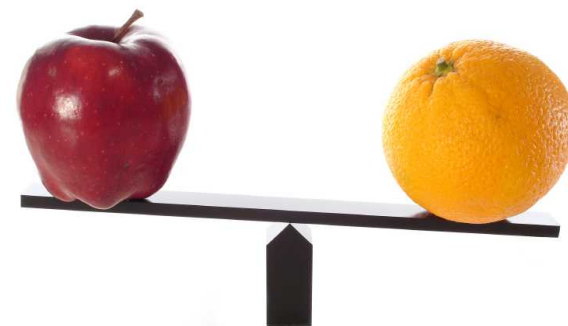
Based on the Collins-Wilczek-Zee (CWZ) Renormalization Scheme
... hence, extensible to all orders

DGLAP kernels & PDF evolution are pure \overline{MS} -Bar
Subtractions are \overline{MS} -Bar

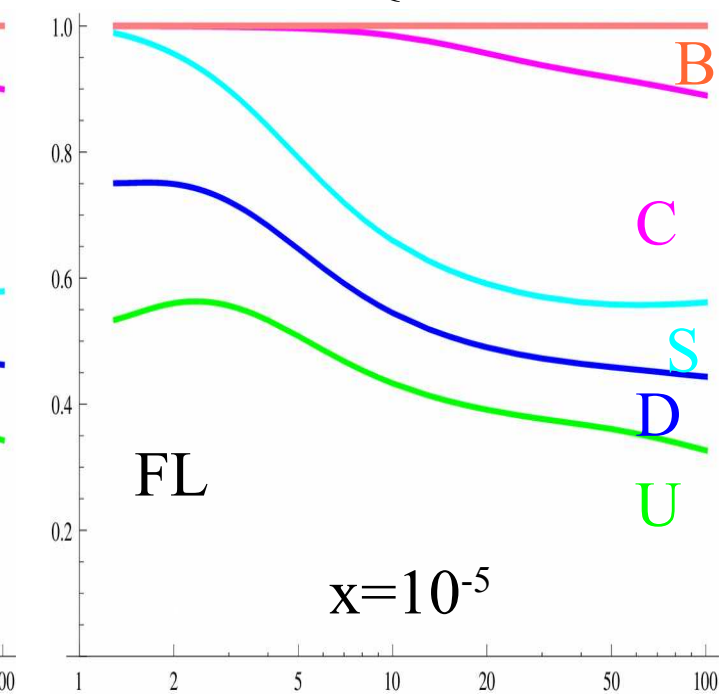
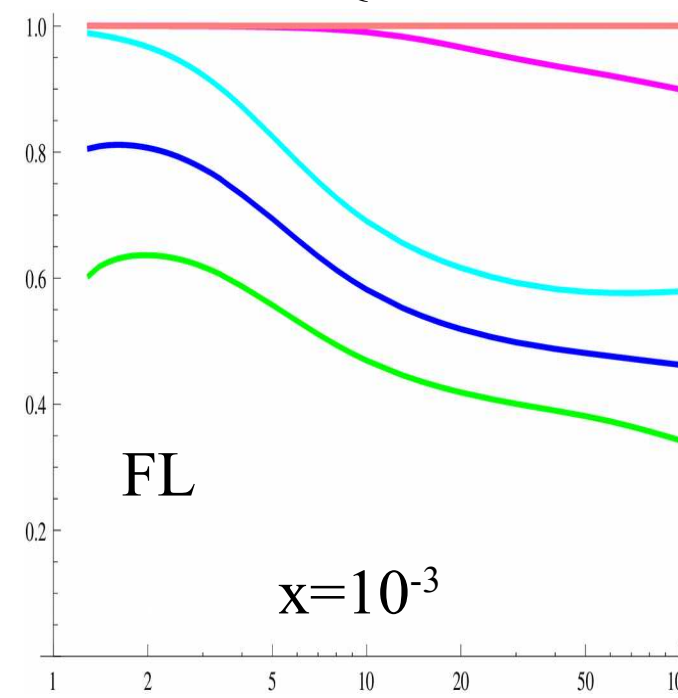
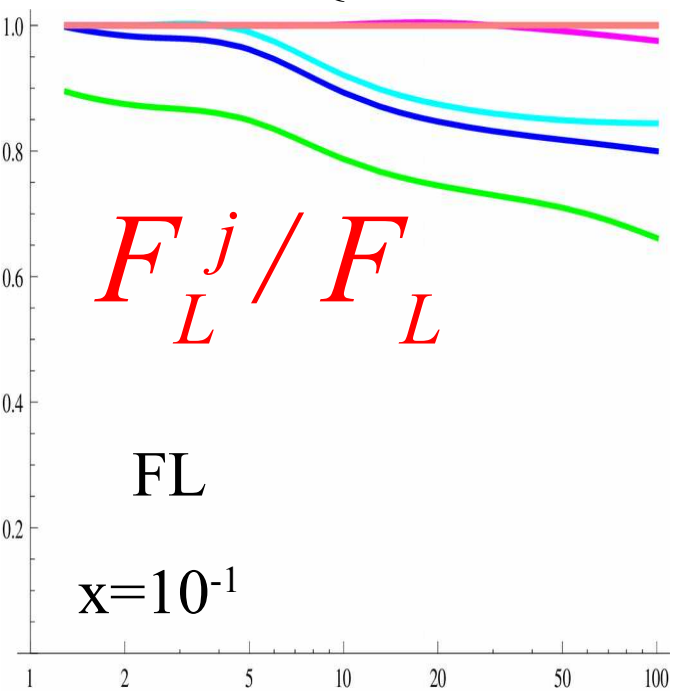
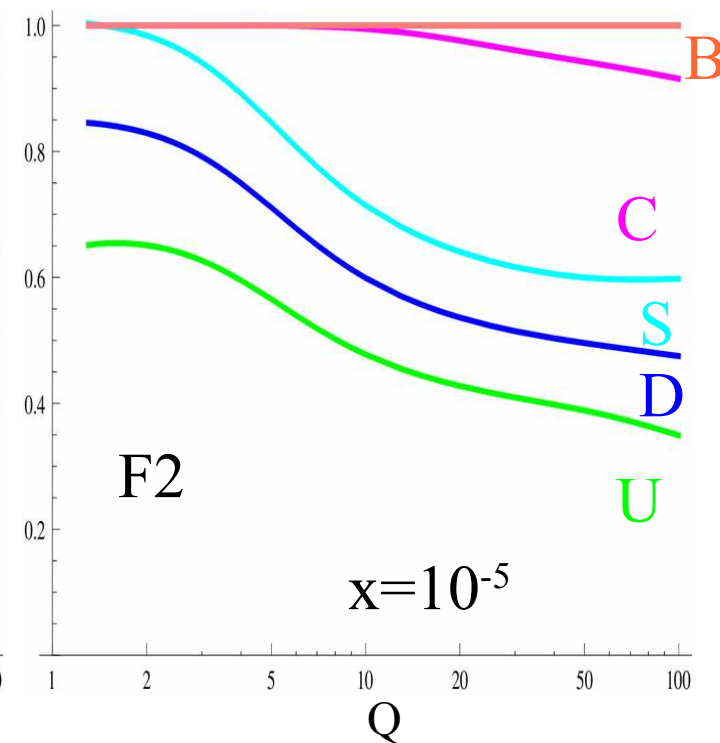
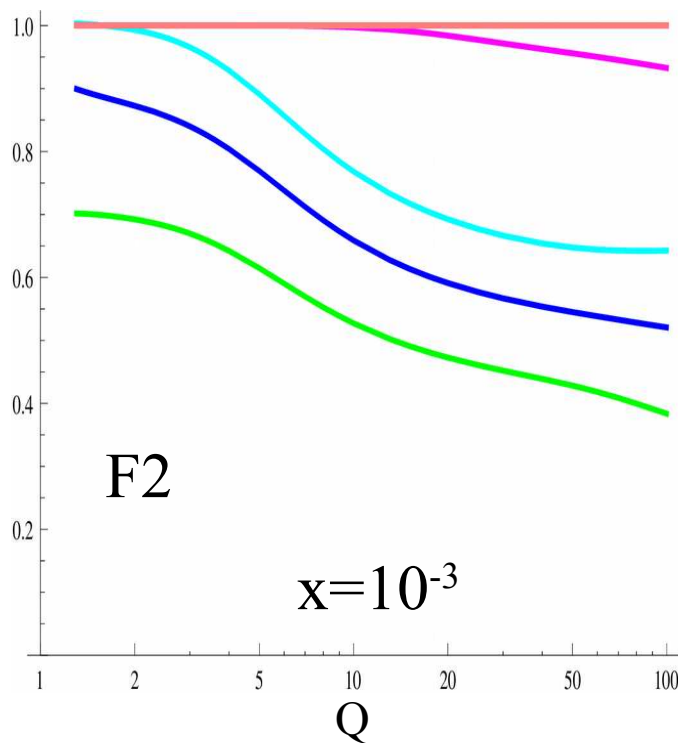
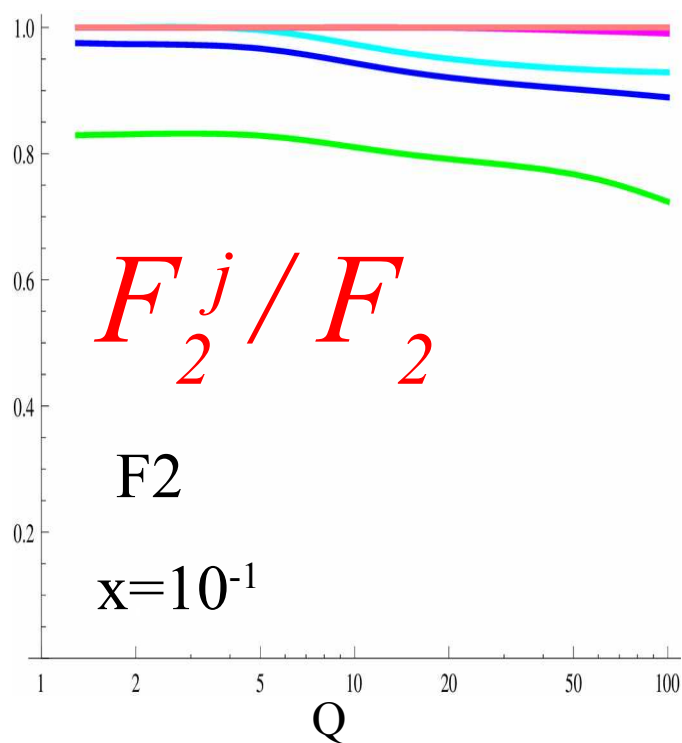
ACOT: $m \rightarrow 0$ limit yields \overline{MS} -Bar
with no finite renormalization

PDFs Discontinuous at N2LO

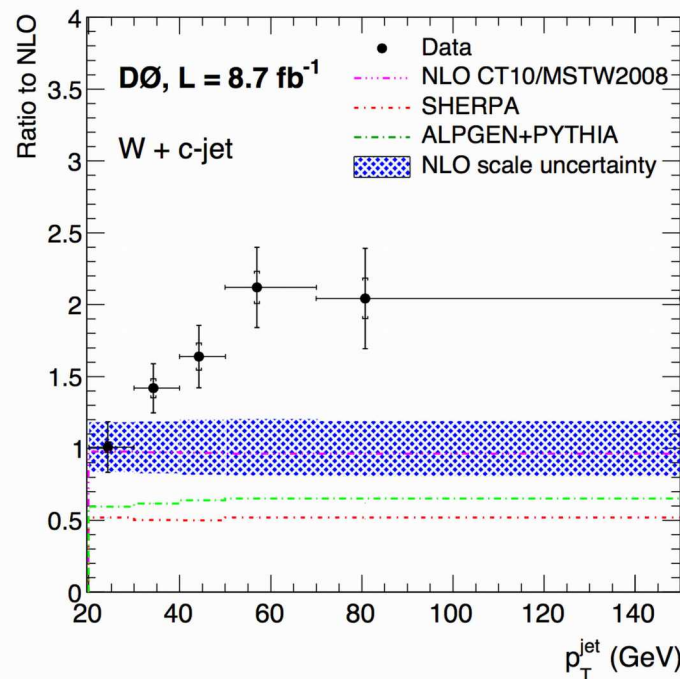
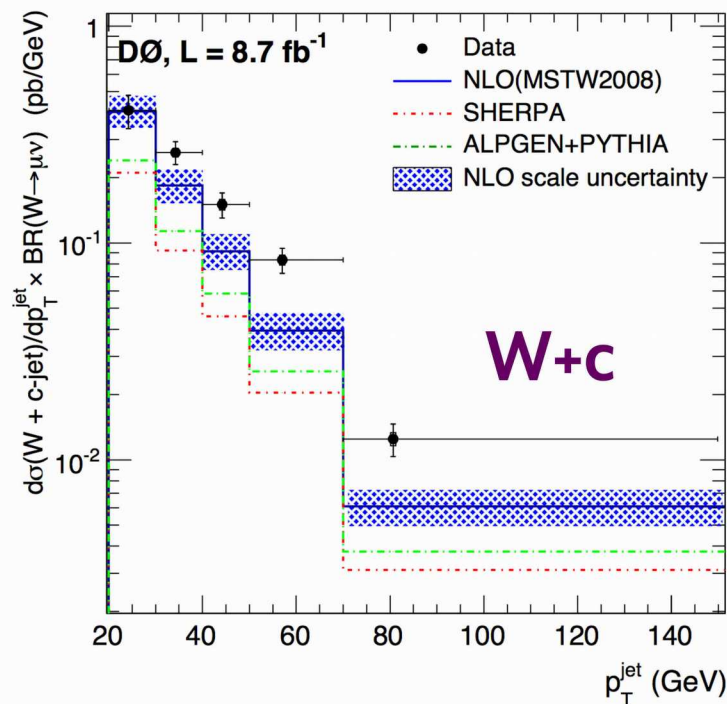
α_s Discontinuous at α_s^3



FLAVOR DECOMPOSITION: Final State Quark:



Extracted W+c production rates corrected for efficiency and acceptance:
4–7% statistical and 12–17% systematic uncertainties, dominantly from c/b-jet ID, selection efficiency, and luminosity



Cross-section compared to predictions from NLO pQCD (corrected for non-perturbative effects), and Sherpa/AlpGen+Pythia MC models.

Unlike W+b, see a clear trend developing to higher jet p_T
High p_T range where gluon splitting becomes increasingly important.

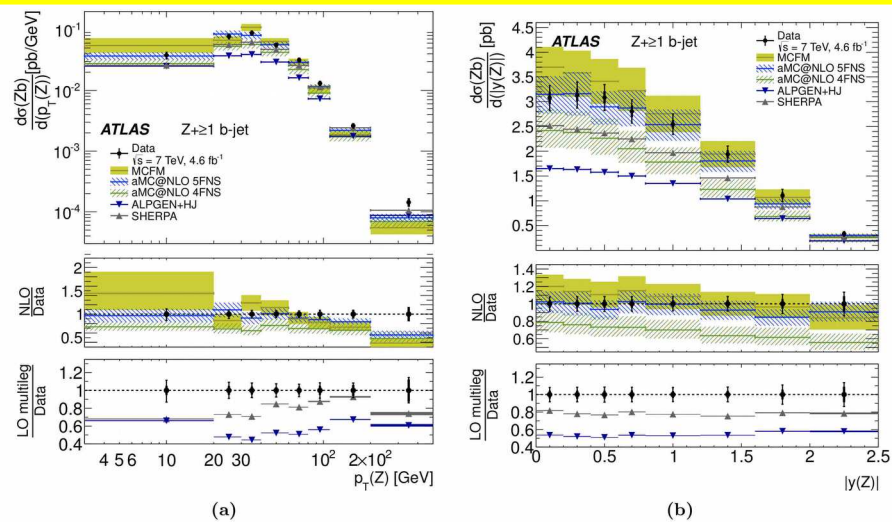


Figure 8. The cross-section $\sigma(Zb)$ as a function of Z boson p_T (a) and $|y|$ (b). The top panels show measured differential cross-sections as filled circles with statistical (inner) and total (outer bar) uncertainties. Overlaid for comparison are the NLO predictions from MCFM and aMC@NLO both using the MSTW2008 PDF set. The shaded bands represents the total theoretical uncertainty for MCFM and the uncertainty bands on aMC@NLO points represent the dominant theoretical scale uncertainty only. Also overlaid are LO multi-legged predictions for ALPGEN+HERWIG+JIMMY and SHERPA. The middle panels show the ratio of NLO predictions to data, and the lower panels show the ratio of LO predictions to data.

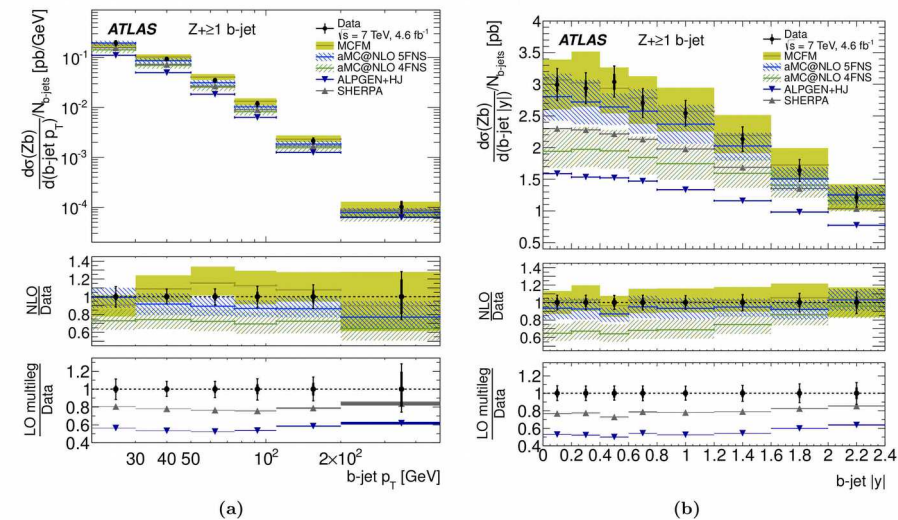


Figure 7. The inclusive b -jet cross-section $\sigma(Zb) \times N_{b\text{-jets}}$ as a function of b -jet p_T (a) and $|y|$ (b). The top panels show measured differential cross-sections as filled circles with statistical (inner) and total (outer bar) uncertainties. Overlaid for comparison are the NLO predictions from MCFM and aMC@NLO both using the MSTW2008 PDF set. The shaded bands represents the total theoretical uncertainty for MCFM and the uncertainty bands on aMC@NLO points represent

ArXiv ePrint: 1407.3643
 Measurement of differential production cross-sections for a Z boson in association with b -jets in 7 TeV proton-proton collisions with the ATLAS detector

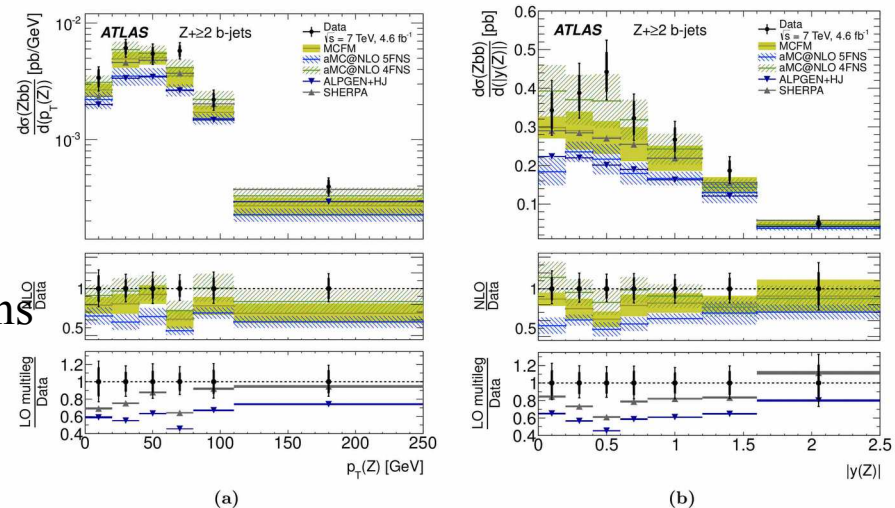


Figure 11. The cross-section $\sigma(Zbb)$ as a function of Z boson p_T (a), and $|y|$ (b). The top panels show measured differential cross-sections as filled circles with statistical (inner) and total (outer bar) uncertainties. Overlaid for comparison are the NLO predictions from MCFM and aMC@NLO both using the MSTW2008 PDF set. The shaded bands represents the total theoretical uncertainty for MCFM and the uncertainty bands on aMC@NLO points represent the dominant theoretical scale uncertainty only. Also overlaid are LO multi-legged predictions for ALPGEN+HERWIG+JIMMY and SHERPA. The middle panels show the ratio of NLO predictions to data, and the lower panels show the ratio of LO predictions to data.

Measurement of the cross-section for W boson production in association with b-jets in pp collisions at $\sqrt{s} = 7$ TeV with the ATLAS detector

$\sqrt{s} = 7$ TeV with the ATLAS detector

JHEP 06 (2013) 084

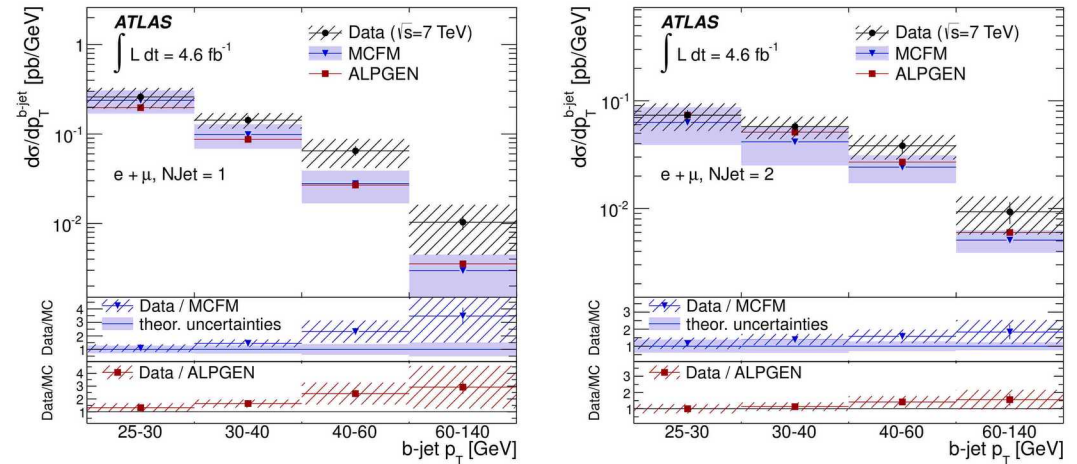


Figure 8. Measured differential $W+b$ -jets cross-sections with the statistical plus systematic uncertainties as a function of $p_T^{b\text{-jet}}$ in the 1-jet (left) and 2-jet (right) fiducial regions, obtained by combining the muon and electron channel results. The measurements are compared to the MCFM predictions and to the ALPGEN predictions interfaced to HERWIG and JIMMY and scaled by the NNLO inclusive W normalization factor. The ratios between measured and predicted cross-sections are also shown.

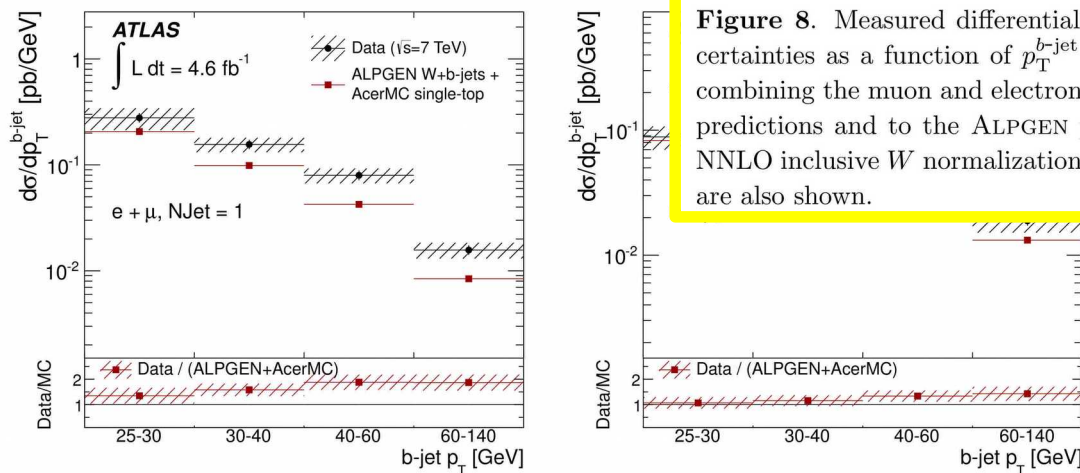


Figure 9. Measured differential $W+b$ -jets cross-section without single-top subtraction as a function of $p_T^{b\text{-jet}}$ in the 1-jet (left) and 2-jet (right) samples, obtained by combining the electron and muon channels. The measurements are compared to the $W+b$ -jets plus single-top predictions obtained using ALPGEN interfaced to HERWIG and JIMMY and scaled by the NNLO inclusive W normalization factor plus ACERMC interfaced to PYTHIA and scaled to the NLO single-top cross-section. The ratios between measured and predicted cross-sections are also shown.

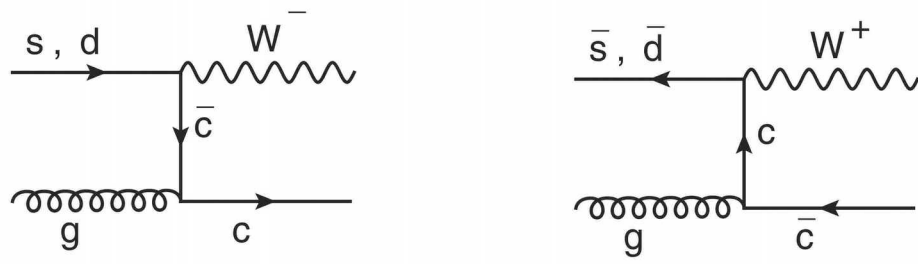


Figure 1. Main diagrams at the hard-scattering level for associated $W + c$ production at the LHC.

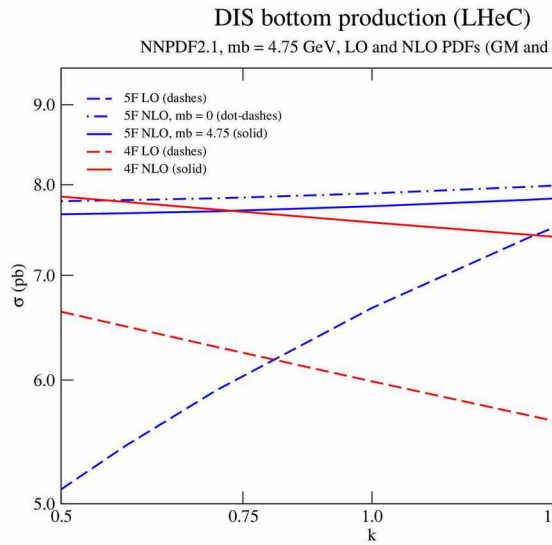
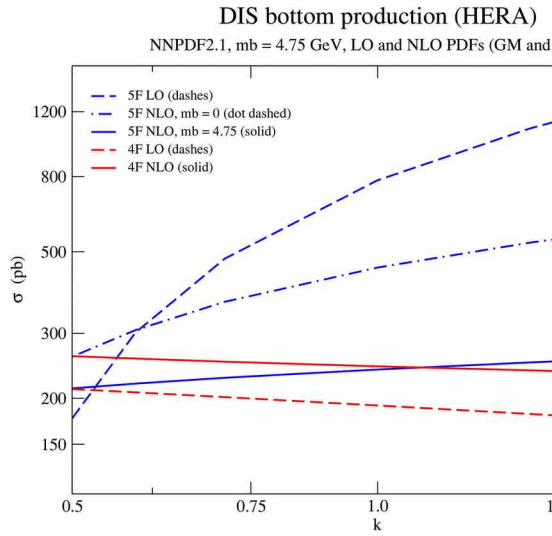


Figure 3. Comparison between 4F and 5F production for $b\bar{b}$ production at HERA (top) and LHeC (bottom). Input PDFs: NNPDF2.1_FF4 (LO and NLO) and NNPDF2.1 (LO and NLO) for the 5F scheme (run with $m_b = 4.75$ GeV, $k = \mu/\sqrt{Q^2 + 4m_b^2}$, with $\mu = \mu_F = \mu_R$).

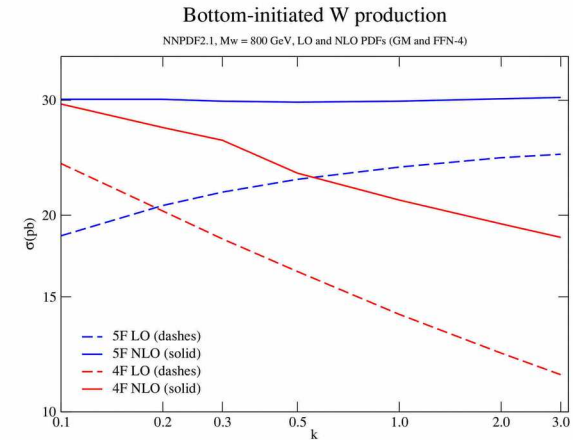
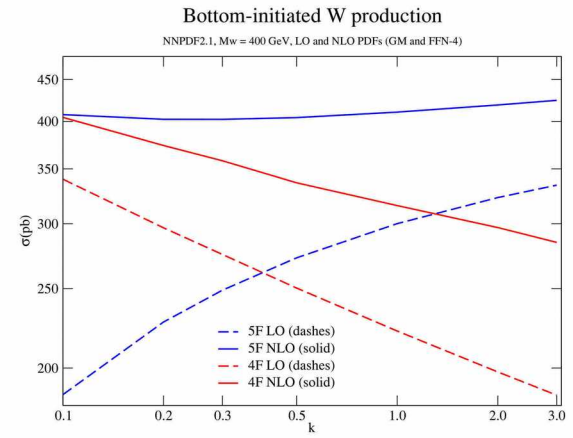
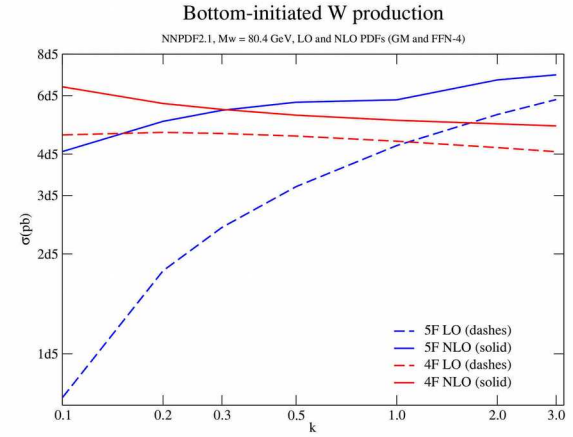


Figure 6. Comparison between 4F and 5F production for b -initiated W production at LHC 14 TeV, for $M_w = 80.4$ GeV (top), $M_w = 400$ GeV (middle), and $M_w = 800$ GeV (bottom).